KYOTO UNIVERSITY

DOCTORAL THESIS

Model-independent study on the internal structure of exotic hadrons

Yuki Kamiya

A thesis submitted in fulfillment of the requirements for the degree of Doctor of Physics

February 4, 2019

Abstract

One of the most significant achievements in recent hadron physics is the discovery of many candidates of exotic hadron states, which are not assigned to the simple $q\bar{q}$ meson nor qqq baryon. By identifying their internal structure and acquiring the knowledge of the favored quark configuration, the understanding of the non-perturbative region of the quantum chromo dynamics (QCD) can be gradually deepen. In this thesis, we develop two different methods to study the internal structure of the candidates of the exotic hadrons from the quantities uniquely determined by the experimental observables and discuss the nature of several exotic hadron candidates .

In the first part of this theses, we focus on the Weinberg's weak-binding relation between experimental observables and a quantity indicating the amount of the dynamical fraction in the hadron state, so called compositeness. Aiming at the application to the actual hadrons, we extend the relation for general cases. With the extended weak-binding relation, we show that the compositeness of the unstable quasibound state can be determined directly from the experimental observables if the eigenstate lies close to the threshold. In the second part, we discuss the relation between the analytic structure of the scattering amplitude and the origin of an eigenstate. Based on the topological nature of the phase of the scattering amplitude, we show that the pole originating in the hidden channel is accompanied by a nearby Castillejo-Dalitz-Dyson (CDD) zero. We develop the method to distinguish the origin of the eigenstate from the positions of the pole and zeros of the amplitude. In the last part, applying the developed methods to actual hadrons, we discuss the structure of $\Lambda(1405)$, $a_0(980)$, $f_0(980)$ and $N\Omega$ dibaryon.

Acknowledgments

I wish to express my utmost gratitude to my supervisor, Professor Tetsuo Hyodo, for patiently instructing me and instilling in me the fascination for hadron physics. I was very fortunate to be able to study under him for five years. I would also like to thank my collaborators, Professor Shung-Ichi Ando, Professor Udit Raha and Doctor Takayasu Sekihara. Thanks to the collaboration with them, I was able to engage in a wide range of research topics. In addition, I would like to thank Professor Atsushi Hosaka, Professor Emiko Hiyama, Professor Hideko Nagahiro, Professor Akinobu Dote, Professor Shigehiro Yasui and Doctor Yasuhiro Yamaguchi for their interest in our research. Finally, I thank all the members of the nuclear theory group at the Yukawa Institute for Theoretical Physics and the physics department of Kyoto University for all their help and encouragement. This work was supported by JSPS KAKENHI Grants No. JP17J04333.

Contents

Chapter 1

Introduction

In this chapter, we first review the current status of the study on the exotic hadrons in Sect. 1.1. In Sect. 1.2, we show how we can investigate the structure of the exotic hadron candidates from the experimental observables without the theoretical ambiguity. Finally, we summarize the motivation and purpose of this thesis in Sect. 1.3.

1.1 Exotic hadrons

Motivated by the discovery of many hadron states [1], the study on the internal structure of hadrons is one of the most fundamental subjects in hadron physics. It can be said that the constituent quark model [2, 3] is the most successful one among the frameworks that explain the internal structure of hadrons proposed to date. In this model, the valence quark q with the baryon number $B = 1/3$ and antiquark $\bar{q}$ with $B = -1/3$ are the fundamental particles. Hadrons are described as the composite state of these particles. The particles composed of three quarks qqq with $B = 1$ are called baryons and those composed one quark and one antiquark $q\bar{q}$ with $B = 0$ are called mesons. In Ref. [4, 5], it is shown that the quark model can describe the property of most of the excited states. This success of the quark model implies that, for the internal structure of most of hadrons, the most favored excitation of the state is the excitation of the constituent quarks.

On the other hand, some of the excited hadrons do not agree with the prediction of the quark models. For the internal structure of these states, the quark configurations other than the simple qqq or $q\bar{q}$ state plays an important role. An example of such states is the excited state of the Λ baryon with spin-parity $J^P = 1/2^-$ called $\Lambda(1405)$. As we will see later, it is considered that the $\bar{K}N$ molecular picture is better to describe this state rather than the compact three quark picture. Such a hadron state, which has the quark configuration other than the simple qqq or $q\bar{q}$, is called exotic hadron.[1] The possibility of exotic states has been discussed from the early stage of the hadron physics ($\sim$1970's) and various candidates are proposed; for example, tetraquarks and pentaquarks which are compact states with four quarks $qq\bar{q}\bar{q}$ and five quarks $qqqq\bar{q}$, respectively, hadron-hadron molecules which are the bound or resonance states of a pair of hadrons, glueball states which are bound states of gluons, hybrid states which contain the gluonic excitation, baryonia which are bound states of the baryon and the anti-baryon.

To identify such exotic states is the fundamental step in studying the quantum chromo dynamics (QCD). By identifying the internal structure of the one of exotic hadrons, we can know which kind of the internal excitation is favored for the states. By acquiring the knowledge of the favored configuration for the various hadron states with the different quantum numbers, the understanding of the non-perturbative region of the QCD can be gradually progressed. Furthermore, the development of physics has been promoted by extracting the fundamental degrees of freedom. In this sense, to elucidate the fundamental degrees of freedom to describe the hadrons is a natural step for the hadron physics.

In the latter part of this section, we review the current understanding of the some of the candidates of exotic hadrons.

1.1.1 Exotics in light sector

The hadron spectroscopy in the light quark sector, which does not include charm c nor bottom b quark, has been studied for a number of decades experimentally and theoretically and various resonance states are detected. As shown in Ref. [4], the internal structure of the most of them can be described well by the constituent quark model. However, there are some long standing problems on the structure of hadrons. Let us review some examples of these exotic candidates and see why these states are considered as the candidates of the exotic hadrons.

[1] There are various ways to define the exotic hadrons. One of them is to define the exotic hadrons as the states which cannot be assigned to qqq baryon, $q\bar{q}$ meson, nor their composite state.

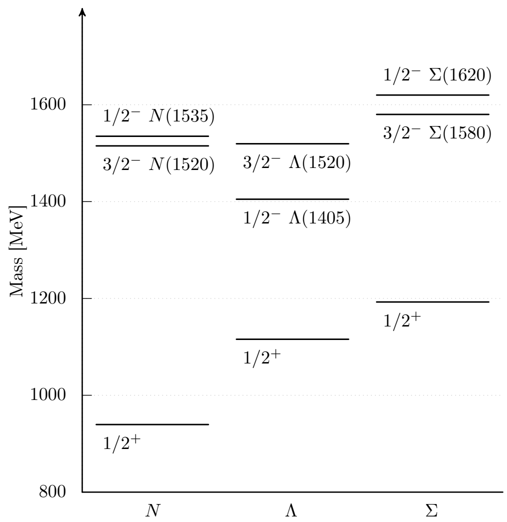

Figure 1.1: Mass spectra of the nucleon, Λ and Σ baryon and their excited states with $J^P = 1/2^-$ and $J^P = 3/2^-$.

One of the long standing problems is the structure of $\Lambda(1405)$, which is the baryon with spin-parity $J^P = 1/2^-$, isospin $I = 0$ and strangeness $S = -1$ [1]. The existence of this state is theoretically predicted in 1959 in Refs. [6, 7] and experimentally confirmed in 1961 in Ref. [8]. From the quantum numbers, $\Lambda(1405)$ is assigned as an excited state of the Λ ground state. However, this state has much lighter mass compared to the other $J^P = 1/2^-$ baryons like $N(1535)$ or $\Sigma(1620)$ (See Fig. 1.1 for illustration.). Especially, it is unnatural that, while this state has the strange quark s whose mass is much heavier than light quarks (u and d), its mass is much lighter than $N(1535)$ with $S = 0$. Furthermore, among the $J^P = 1/2^-$ baryons, this state only has sizably $\gtrsim 100$ MeV lighter mass than the mass of its spin-orbit partner, $\Lambda(1520)$ with $J^P = 3/2^-$, whereas the mass splitting of the partners is less than 50 MeV for other pairs. Such unnaturally light mass implies that $\Lambda(1405)$ is not a simple qqq baryon but an exotic hadron state.

To discuss the internal structure of a hadron, its mass and decay width provide the fundamental information. Generally, a bound or resonance state is represented by a pole of the scattering amplitude in the complex energy plane. For typical resonances, the real (imaginary) part of the pole corresponds to the position (half width) of the peak structure of the invariant mass distribution or the cross section. However, the recent studies on the

$\Lambda(1405)$ baryon reveal that such a simple correspondence between the pole position and the peak structure does not hold for this baryon and the peak of the $\Lambda(1405)$ is generated by the two resonance poles in the complex energy plane [9–12]. Of these, one close to the $\bar{K}N$ threshold is called high-mass pole and the other close to the $\pi\Sigma$ threshold is called low-mass pole [1]. This means that there are two eigenstates corresponding to these two poles. Besides the problem of the internal structure of the eigenstates, the two-pole structure of $\Lambda(1405)$ itself is an interesting topic. For the study of the internal structure of hadrons, we have to investigate the structure of each state. The structure of the $\Lambda(1405)$ is discussed in Chapter 4.

Other candidates are the $J^P = 0^+$ lightest scalar mesons. $f_0(980)$ and σ with isospin $I = 0$, κ with $I = 1/2$ and $a_0(980)$ with $I = 1$ form $J^P = 0^+$ nonet. The experimental values of masses of these mesons satisfies the following relations;

$$m(\sigma) < m(\kappa) < m(a_0(980)) \cong m(f_0(980)). \tag{1.1.1}$$

The masses of $f_0(980)$ and $a_0(980)$ are larger than those of the other states. This is unnatural because the masses of the κ mesons, which include s or $\bar{s}$ quark, should be larger than the mass of $a_0(980)$ and that of one of two $I = 0$ states if we assume the ideal mixing. Considering that the description of quark models for the 1^+ nonet works well, the relations among the masses of the 0^+ mesons tell us that at least some of them are not the simple $q\bar{q}$ state. Furthermore, the large mass splittings between the 0^+ mesons and 2^+ mesons are inconsistent with the prediction of quark models. In constituent quark models, these mass splittings originates in the spin-orbit (LS) force. Compared to the mass splittings between the $1/2^-$ baryon and the $3/2^-$ baryon 10-20 MeV, which also originate in the spin-orbit force, the experimental values of the mass splittings between the 0^+ mesons and 2^+ are ten times or more lager. Thus, in order to explain this large splitting, some mechanisms other than the *LS* force is needed.

The mass relations among the 0^+ scalar nonets can be explained by assuming that they are composed of four quarks $qq\bar{q}\bar{q}$. This is because the $s\bar{s}$ component comes into the model space and the large masses of $f_0(980)$ and $a_0(980)$ can be explained by the four quark component including $s\bar{s}$ [13]. In Refs. [14, 15], within the quark bag model, it is shown that the masses of the 0^+ nonets can be well described by the compact tetraquark state. The meson-meson molecular picture, which also contains the four-quark configuration in total, for these states are proposed in Ref. [16], and later it has been shown that the chiral dynamics well explains the mass of the $f_0(980)$ and $a_0(980)$ mesons in Ref. [17]. In addition to these discussions, for the $f_0(980)$ meson, the contribution of the glueball, which is a bound state of gluons, is discussed in Ref. [18]. The structure of the $f_0(980)$ and $a_0(980)$ mesons is discussed in Chapter 4.

Hadrons with the baryon number $B = 2$, such as the deuteron, is called dibaryon. The dibaryon other than the deuteron has been predicted theoretically more than 50 years ago [19]. Stimulated by the prediction of H dibaryon, which is a bound state of $\Lambda\Lambda$, by Jaffe [20], the various dibaryon systems have been actively discussed experimentally and theoretically. However, there are no other states found besides the deuteron.

1.1.2 Exotics in heavy sector

Thanks to being able to use the high statistics data with abundant charm c and bottom b quark productions, e.g. the B meson decay data from e^+e^- collision accumulated by B-factory, the hadron spectroscopy in the heavy sector is drastically promoted since around 2000. Among newly detected heavy hadrons, the mesons called XYZ, which have the $c\bar{c}$ (or $b\bar{b}$) component in the internal structure but cannot be assigned as the simple $c\bar{c}$ meson, are the promising candidates of the exotic hadrons [21–23]. The mass of the XYZ states are close to or larger than the threshold energy of $D\bar{D}^*$ or $B\bar{B}^*$ channel. This implies that the degree of the four-quark component $c\bar{c}q\bar{q}$ may play an important role for the internal structure of these states.

Among the XYZ particles, the state which is the most studied experimentally and theoretically is $X(3872)$, which is firstly detected by the narrow peak in the $J/\psi\pi^+\pi^-$ mass spectrum from the B meson decay by the Belle collaboration [24]. The reason why this state is not assigned to the simple $c\bar{c}$ state is due to the too small experimental value of the decay width (< 1.2 MeV), while the prediction of the quark model is hundred times or more larger than this value (~ 130 MeV) [25]. Due to the mass of this state which is very close to the $D\bar{D}^*$ and $D^*\bar{D}$, the $D\bar{D}^*$-$D^*\bar{D}$ molecule is the most promising candidate for the structure of $X(3872)$. However, the compact tetraquark state is also possible structure for this state.

1.1.3 New approaches to hadron structure

In hadron spectroscopy for exotic hadrons, partial wave analyses of scattering data and analyses of invariant mass distribution in the decay process are standard techniques. However, in future studies, new theoretical and experimental approaches may be used to study the spectroscopy for exotics hadrons.

With the recent advancement of the numerical calculation technique, the lattice QCD calculation, which is the first principle numerical calculation of the QCD in the discrete Euclidean space-time, is beginning to be used to study exotic hadrons. Most of the lattice QCD calculations are performed with the unphysical quark mass, where the hadron masses are much heavier than that of the experimental values, because the numerical cost is much cheaper than the calculation at the physical point, where the mass of the pion is almost its physical value ≈ 140 MeV, However, in the recent years, the results of the QCD calculation at the physical point has been reported and the obtained masses of the various hadrons show the good agreement with the experimental values [26, 27].

Another way is to study the two-hadron intensity correlation in the heavy-ion collisions [28–36], which is generated by the effect of quantum statistics and the final state interaction. The former one is called Hanbury–Brown and Twiss (HBT) [37] or Goldhaber–Goldhaber–Lee–Pais (GGLP) [38] effect, which can give information on the source size from (anti-)symmetrization of the two-boson (fermion) wave function. The correlation of the particle pairs with strong interaction in the range of the source size is expected to be significant [30, 31]. Once the effective source size has been given from the quantum statistical effect of stable hadrons, the pairwise interaction of non-identical hadron pairs, where the quantum statistical effect does not exist, can be studied by the measurement of the correlation function with the high statistics. This technique is very useful in particular for the channel whose interaction is difficult to study through the scattering experiments. It is also pointed out that, compared to the scattering experiments, the hadron-hadron correlation gives the complementary information [39–41], especially for the coupled-channel systems [42, 43]. Furthermore, the low energy region of the interaction, which is difficult to approach in the scattering amplitude, can be accessed through the correlation.

1.2 Methods to investigate the structure from the scattering amplitude

To distinguish the internal structure of the hadrons is not a simple task due to the difficulties as follows. Firstly, two or more configurations with the same quantum numbers can make a mixed state. For example, the quantum numbers of $\Lambda(1405)$ can be described by any quark configurations such as a genuine pentaquark state ($sqqq\bar{q}$), a composite state of a $\bar{K}$ meson ($s\bar{q}$) and a nucleon (qqq) and a simple three-quark state (sqq). In this case, we cannot distinguish the structure by the quantum numbers and we have to prepare a good "discriminator" that tells us which component is dominant.

Secondly, model ambiguity may arise when we discuss the structure from the result of the model calculation. A model can be constructed by preparing the model space and by tuning the free parameters to reproduce the experimental data. In the latter procedure, the contribution of the degrees of freedom that are excluded from the model space may unintentionally come into the obtained model via the fitted free parameters. Thus, even when the model reproduces the experimental data well, it is not clear whether the employed degrees of freedom is suitable [44, 45].

To avoid such difficulties, we can discuss the structure based on the quantities that can be in principle determined uniquely from the experimental observables. One of such physical quantities is the on-shell scattering amplitude, which has the various information of the scattering system. Thus, by deriving the relation between the scattering amplitude and internal structure of hadrons, we can discuss the hadron internal structure in a model-independent manner. Thanks to the progress of research on interaction in recent years, it is gradually becoming possible to determine the scattering amplitude. This fact also ensures that we can develop the method to distinguish the exotic hadron structure from the scattering amplitude.

In this section, we firstly review the important characteristics of the scattering amplitude and its pole position. We also discuss that the energy where the amplitude vanishes is also important for the study of the hadron structure. After that, we review the method to distinguish the structure of the eigenstate from these quantities proposed previously.

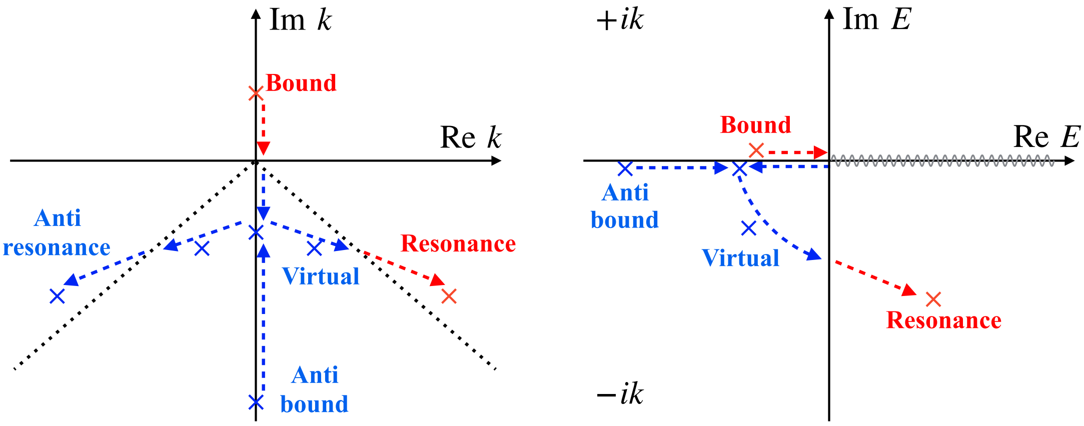

Figure 1.2: The trajectories of the poles in the s-wave amplitude in the complex k-plane (left panel) and E-plane (right panel). The red cross denotes the physical pole which represents the physical eigenstate while the blue close denote the unphysical pole.

1.2.1 Pole of amplitude

To discuss the property of hadrons, one of the most important quantities is the pole energy of the scattering amplitude. While its position is in the complex energy plane, this is a model-independent quantity because the analytic continuation to the complex energy plane is in general unique.[2] The pole energy is nothing but the eigenenergy of the eigenstate [46].

Let us review the relation between the pole position in the near-threshold region and the threshold parameters in the nonrelativistic treatment. In the case of the single channel problem, the physical eigenstate is simply classified as a bound state or a resonance state. The bound state has the negative eigenenergy $E_B < 0$, where we take the origin of energy at the threshold energy, and pure imaginary eigen-momentum Re $k_B = 0$. The imaginary part of the eigen-momentum must be positive Im $k_B > 0$ because the radial wave function of the eigenstate, that behaves as $r\psi(r) \sim \exp(ik_B r)$ at the large distance, must be normalizable. On the other hand, the resonance state has the complex eigenenergy E_R which satisfies Re $E_R > 0$ and Im $E_R < 0$. Correspondingly, its eigen-momentum k_R satisfies Re $k_R > -$Im k_R and Im $k_R < 0$. Note that the expectation value of any operator can be

[2]In practice, due to the uncertainty of the experimental data, the scattering amplitude determined by analyzing the data also has uncertainty.

complex value for the resonance state due to the nature of the non-Hermite systems [47]. Even though the Hamiltonian includes only the real potential, the non-Hermiticity may arise through the boundary condition. The complex value of the expectation value is troublesome when we discuss the nature of the resonance state, e.g. the mean square radius of the resonance state.

The pole position in the complex momentum plane corresponds to the eigen-momentum one to one. However, when we consider the pole position in the complex energy plane, we have to be careful about the choice of the Riemann sheet. Because the eigen-momentum k is related to the energy E as $k = \pm\sqrt{2\mu E}$, there are two choices of eigen-momentum for any energy E. We call the Riemann sheet which corresponds to the upper (lower) half of the momentum plane as the first (second) sheet. Then the pole representing the bound (resonance) state lies on the first (second) Riemann sheet.

The poles discussed above represent the physical eigenstate. However, in the complex $k(E)$-plane, there may exist a pole which does not correspond to the physical eigenstate, so called virtual state in the region $\mathrm{Re}\ k_p < |\mathrm{Im}\ k_p|, \mathrm{Im}\ k_p < 0$. Furthermore, when the resonance pole E_R (p_R) emerges, the conjugate pole must emerge at $E = E_R^*$ in the upper half of the first sheet of the E-plane and at $p = -p_R^*$ in the k-plane. This is because the amplitude satisfies $\mathscr{F}_l(-p^*) = \mathscr{F}_l(p)$ due to the unitarity of the scattering matrix [48].[3]

It is instructive to see the pole trajectory in the near-threshold energy region when we vary the strength of the interaction. To discuss the behavior of the low energy scattering problem with the short range interaction, it is convenient to utilize the effective range expansion (ERE) of the scattering amplitude which is given as

$$\mathscr{F}_l(k) = \frac{k^{2l}}{-\frac{1}{a_l} + \frac{r_l}{2}k^2 + \mathscr{O}(k^4) - ik^{2l+1}}, \tag{1.2.1}$$

where l denotes the angular momentum, a_l and r_l are the threshold parameters called scattering length and effective range, respectively.[4] Due to the unitarity of the scatter-

[3] This can also be shown as follows. When the state $|\psi\rangle$ is the eigenstate of full Hamiltonian of the system with eigenenergy E_R as $H|\psi\rangle = E_R|\psi\rangle$, the state $|\psi^*\rangle$, whose wave function is the complex conjugate of the wave function of $|\psi\rangle$, is also the eigenstate but with the eigenenergy E_R^* if the Hamiltonian includes real potential.

[4] Both a_l and r_l have the dimension of length to the power of $1-2l$. Only for s-wave ($l = 0$), a_l and r_l have the dimension of "length".

ing matrix, these threshold parameters are real and the imaginary part of the scattering amplitude on the physical energy region is introduced only through the term of $-ik^{2l+1}$.

Now let us assume that the system has one stable s-wave bound state with small binding energy. For sufficiently small binding energy, the pole position is determined only by the positive and large scattering length as

$$k_{\text{pole}} = \frac{i}{a_0}. \tag{1.2.2}$$

In this case, only one length scale, a_0, governs this system and the system has the universality. By decreasing the strength of the interaction, the binding energy decreases and then it becomes zero ($k_{\text{pole}} = 0$). This limit, where the zero energy resonance emerges $k_{\text{pole}} = 0$ and the scattering length diverges $a_0 = \infty$, is called the unitary limit. By decreasing the interaction a bit further, pole moves from the upper half to the lower half in the k-plane or moves first sheet to second sheet in the E-plane and the scattering length changes the sign from $+$ to $-$ (See Fig. 1.3.). At this moment, the pole no longer represents the physical state and becomes the virtual pole. By decreasing the interaction further, the pole moves on the real axis of the E-plane and imaginary axis on the k-plane as long as $|a_0|$ is large.

As we further weaken the interaction, Eq. (1.2.2) fails to describe the pole position and the contribution of the effective range r_0 must be taken into account as

$$k_{\text{pole},\pm} = -\frac{i}{r_0} \pm \frac{1}{r_0}\sqrt{-1 - \frac{2r_0}{a_0}} = \frac{i}{r_0}\left(-1 \pm \sqrt{1 + \frac{2r_0}{a_0}}\right). \tag{1.2.3}$$

When a_0 equals to r_0, the scattering amplitude has the pole of order 2 at $k_{\text{pole}} = -i/r_0$. This occurs by overlapping the pole that has been the bound state pole and the other pole that has moved upwards on the imaginary axis from the bottom in the k-plane, which is called antibound state. Thereafter, the second order pole is separated into one pole moving to the right and the other pole moving to the left. Of these two poles, the former may become the resonance pole when the Re k_{pole} exceeds $|\text{Im}\, k_{\text{pole}}|$. The trajectories of the poles in the k-plane and E-plane are shown in Fig. 1.2.

The trajectory of the pole representing the near-threshold state with higher angular momentum ($l \geq 1$) weakening the interaction is qualitatively different. Firstly, even though the scattering length is so large; $a_l \gg r_l$, we need the effective range to discuss the bound state, because the subleading term of the ERE is no longer the term of $-ik^{2l+1}$ but $r_l k^2/2$. The effective range r_l is always nonnegligible for the scattering with $l \geq 1$ due to

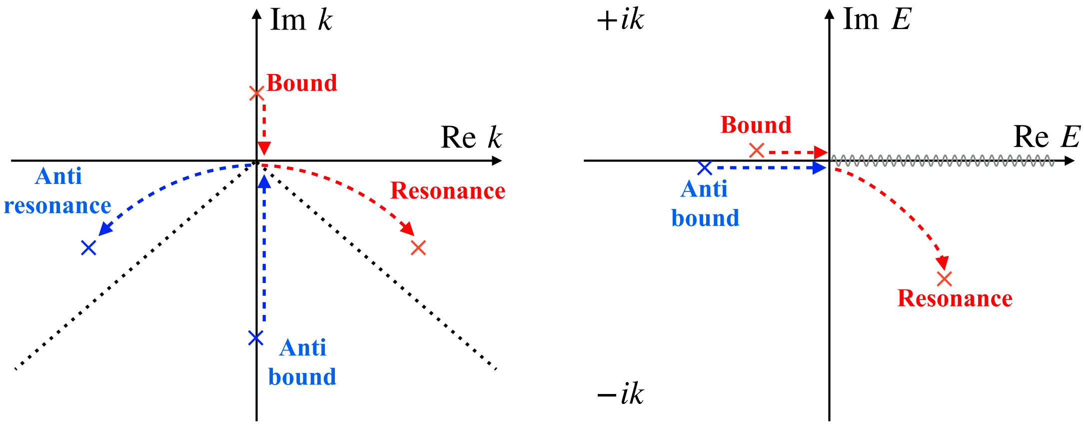

Figure 1.3: The trajectories of the pole in the higher-partial waves $l \geq 1$ in the complex k-plane (left panel) and E-plane (right panel). The red cross denotes the physical pole which represents the physical eigenstate while the blue close denote the unphysical pole.

the causality [49]. Up to the next leading-order term of the expansion, the positions of the poles are written as

$$k_{\text{pole},\pm} = \pm\sqrt{\frac{2}{a_l r_l}}. \tag{1.2.4}$$

Thus, unlike the s-wave state, the bound state cannot be expressed only with the scattering length and the system is no universal. Secondly, the bound sate pole directly becomes the resonance pole through the zero energy bound pole. With the infinitely large a_l, the denominator of Eq. (1.2.1) is written as $k^2(r_l/2 - ik + \mathscr{O}(k^2))$, which means that the zero energy bound pole must be double. Thus the pair of the resonance pole and its conjugate pole appears from the origin.[5]

Next, let us consider the coupled-channel scattering problem. For any energy E, the eigen-momentum is different for each channel. When we consider the N coupled-channel problem, we have $2N$ Riemann sheets because we have two choices of the sign of the imaginary part of the momentum for each channel. For simplicity, let us consider two-channel problem with one unstable eigenstate. We write the eigen-momentum of channel i as k_i and the Riemann sheet with Re $k_1 > 0$ and Re $k_2 < 0$ as $(1,2)$ sheet. We assume that

[5]Note that, for the single channel problem, the pole and its conjugate pole must appear by the separation of the second order pole at the point on the imaginary axis.

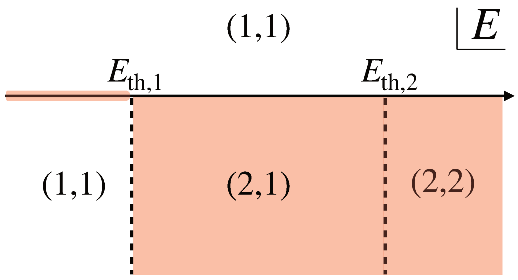

Figure 1.4: The adjacent Riemann sheets to the physical real energy in the two-channel problem. The region where the physical pole may lie is shown with the red shadow.

the threshold energy of channel 2 is higher than that of channel 1. The most adjacent Riemann sheets to the physical energy region are explained in Fig. 1.4. The pole representing the physical eigenstate can appear in the energy region shown in Fig. 1.4. Note that the position of the pole is common to all of the components of the scattering amplitude $\mathscr{F}_{ij}$.

Now let us consider the case where the eigenstate appears near to the threshold energy of the channel 2 $E_{\text{th},2}$. In this case, the relevant Riemann sheets are $(2,1)$ sheet and $(2,2)$ sheet so we just consider the poles on these sheets. As done in the single channel problem, the effective range expansion (1.2.1) is useful to describe the scattering amplitude of channel 2 $\mathscr{F}_{22}$ in the near-threshold region while the threshold parameters a_l and r_l are complex due to the coupling to the decay channel. When the eigenstate lies lower than $E_{\text{th},2}$, the physical pole appears in the $(2,1)$ sheet. We call such eigenstate quasibound state.[6] Again its pole position is well approximated by Eq. (1.2.3). As we weaken the interaction of channel 2, the real part of the pole energy reaches the threshold of channel 2 and become the unphysical pole. At this time, as in the case of the single channel problem, the other pole of Eq. (1.2.3) reaches to the threshold energy in the complex energy region. However, in general, these two poles do not encounter with each other in the coupled-channel problem.[7] The trajectories obtained by weakening the interaction further depend on the detail of the interaction.

[6]In most cases, quasibound state originates in the dynamics of channel 2. However, the eigenstate with other origin may accidentally lie close to the threshold.

[7]Note that the conjugate pole appears in the different Riemann sheet.

1.2.2 CDD zero

The Castillegio-Dalitz-Dyson (CDD) zero [50, 51] is defined as the zero of the scattering amplitude: $\mathscr{F}(E_{\mathrm{CDD}}) = 0$.[8] Due to this definition, like the eigenstate pole, the CDD zero can be regarded as the model-independent quantity. As a feature different from the eigenstate pole, the position of the CDD zero is channel-dependent in the coupled-channel amplitude while the position of the pole is common for all the components. Furthermore, the CDD zero can appear at the real energy where the scattering experiment can be performed while any pole should lie in the complex energy plane. This fact is important when we discuss the resonance and its peak structure of the scattering amplitude. The CDD zero on the physical real axis or that lies close to the physical real energy may distort the line shape of resonance peak of the scattering amplitude from the Breit-Wigner form. This is because the amplitude must be equal to zero at this point while the Breit-Wigner amplitude cannot be equal to zero. An example of the CDD zero is the one in the $\pi\Sigma$ amplitude [52]. As shown in Fig. 1.5, the CDD zero lies at the physical energy region in the $\pi\Sigma$ amplitude at $\sqrt{s} = 1428$ MeV while there is no such zero in the $\bar{K}N$ amplitude. Because of such CDD zero, the $\Lambda(1405)$ peak in the $\pi\Sigma$ amplitude is distorted from the Breit-Wigner form.[9]

Unlike a pole, the direct relation between a CDD zero and the feature of the eigenstate is unknown. However, the importance of the CDD zero contribution in the analysis of the hadron scattering amplitude is recognized as follows. In Refs. [53, 54], the general form of the hadron scattering amplitude including the CDD contribution is discussed. The CDD zero effect on the effective range expansion in the near threshold region is discussed in detail for the case of a single channel scattering in Ref. [55] and for the case of multicontinuum channels in Ref. [56]. Recently, the effect of the near-threshold CDD zero is discussed in the study of $\Lambda_c(2595)$ in Ref. [57] and in the study of $X(3872)$ in Ref. [58].

[8] The CDD zero is often referred to as CDD pole because it represents the pole of the inverse amplitude. In this thesis, we call it CDD zero in order to avoid the confusion with the pole of the amplitude.

[9] The distortion of the $\Lambda(1405)$ peak is also caused by the two-pole structure.

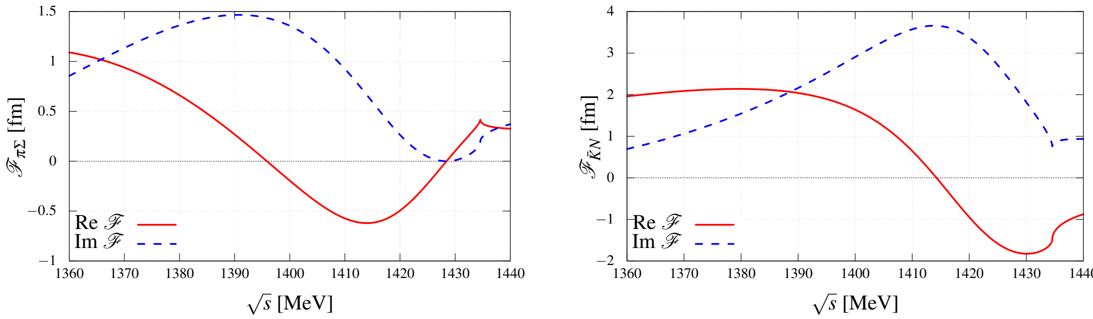

Figure 1.5: The $I = 0$ scattering amplitude in $\pi\Sigma \to \pi\Sigma$ channel (left panel) and $\bar{K}N \to \bar{K}N$ channel (right panel) calculated with the effective Tomozawa-Weinberg model constructed in Ref. [59]. The solid line denotes the real part and the dashed line denotes the imaginary part.

1.2.3 Compositeness

The simplest way to discuss the structure is to quantitatively evaluate the amount of the different components in the eigenstate. Such idea is already introduced more than 50 years ago by Weinberg in order to identify whether the deuteron is an elementary particle or the n-p composite state [60]. In this study, the probability of finding the bare state in deuteron Z, which is called elementariness, is introduced with the wave function of the deuteron. The quantity $X \equiv 1 - Z$, which is nowadays called compositeness, is interpreted as the probability of finding the molecular state of n and p. With the bare state $|n\rangle$ and the bound state $|d\rangle$, the elementariness Z is defined as

$$Z \equiv |\langle n|d\rangle|^2. \tag{1.2.5}$$

By utilizing the solution for the low-energy region of the Low equation, the quantity Z is related to the scattering length a_0 and effective range r_e as

$$a_0 = 2R\frac{1-Z}{2-Z} + \mathcal{O}(m_\pi^{-1}) = 2R\frac{X}{1-X} + \mathcal{O}(m_\pi^{-1}), \tag{1.2.6}$$

$$r_e = -R\frac{Z}{1-Z} + \mathcal{O}(m_\pi^{-1}) = -R\frac{1-X}{X} + \mathcal{O}(m_\pi^{-1}), \tag{1.2.7}$$

where m_π is the mass of the pion and R is the deuteron radius $R = \sqrt{2\mu B}^{-1}$ with binding energy of the deuteron B and the reduced mass of the proton and the neutron μ. The relations (1.2.6) and (1.2.7) are called weak-binding relations.[10] Eqs. (1.2.6) and (1.2.7)

[10]These relations are also called Weinberg's relations or compositeness relations.

are the model-independent relations because they are derived with simple assumption that the interaction of the low-energy region does not strongly depend on the energy. If the binding energy is sufficiently small that the correction term $\mathscr{O}(m_\pi^{-1})$ can be neglected, Z (or X) can be determined directly from one of the threshold parameters and the binding energy, which are experimental observables. Thus, we can qualitatively discuss the structure of the eigenstate directly from the experimental observables.

For the deuteron, using the experimental values of the threshold parameters and the binding energy, it is shown that $a_0 \approx R$ and $r_e = \mathscr{O}(m_\pi^{-1})$, which are consistent with the scenario where the deuteron is the composite state ($Z \sim 0$ and $X \sim 1$) from the weak-binding relations (1.2.6) and (1.2.7). On the other hand, if the deuteron were a compact elementary state with six quarks ($Z \sim 1$ and $X \sim 0$), these experimental values would satisfy $a_0 \approx \mathscr{O}(m_\pi^{-1})$ and $r_e \approx -\infty$. Thus, it has been concluded that the structure of the deuteron is mostly dominated by the *n*-*p* composite state. In Chapter 4, we revisit the structure of the deuteron and discuss the value of compositeness more quantitatively.

The weak-binding relations (1.2.6) and (1.2.7) hold for various eigenstates which satisfy the following conditions;

(i) The eigenstate is the stable bound state:

(ii) The eigenstate is the *s*-wave scattering state:

(iii) The effective range expansion converges well at the eigenstate pole.

In addition to these conditions, in order to determine Z and X from the observables, we need the weak-binding condition;

(iv) The binding energy B is sufficiently small that the correction term in Eqs. (1.2.6) and (1.2.7) can be neglected.

When these four conditions are satisfied, we can model-independently discuss the structure with the Weinberg's factor Z or the compositeness X. In the following, we mainly discuss the determination of the compositeness.[11]

[11] As we will see in Chapter 2, the compositeness X, rather than the elementariness Z, is the fundamental quantity.

Such model-independent discussion based on the experimental observables is preferable for studying the structure of exotic hadrons. However, in order to discuss the structure of exotic hadron candidates more practically with this method, we need the extension of the weak-binding relation for the various cases. Firstly, because the almost all the exotic hadron candidates are unstable, the condition (i) is not satisfied and the weak-binding relations cannot be applied directly.

Secondly, the weak-binding relations cannot be applied when the eigenstate pole accompanied by the CDD zero of the amplitude because the ERE does not converge well and the condition (iii) does not hold in this case. This problem is already mentioned by Weinberg [60]. As we have seen in Sect. 1.2.2, the emergence of such zero is related to the nature of the eigenstate. Thus, for broader applicability, we need to extend the weak-binding relation for the case where the ERE does not converge.

Thirdly, related to the condition (iv), the magnitude of the error of compositeness which comes from the correction term of the weak-binding relation is unclear. In order to discuss the hadron structure quantitatively, we need a method to estimate the error from the experimental observables.

In order to discuss the structure of the exotic hadron candidates using the Weinberg's idea, several approaches for the unstable states have been proposed. In Ref. [61], Weinberg's discussion is extended by introducing the spectral function and show that this function includes a measure of the admixture of the bare state in the physical state. This discussion is later extended to the multichannel case in Ref. [56]. In Ref. [62], Weinberg's weak-binding formula is directly applied to a resonance close to the lowest energy threshold in the convergence region of the effective range expansion. In Ref. [63], it is shown that the compositeness of s-wave states is expressed by the residue of the pole and the derivative of the loop function based on the Yukawa model. A similar expression is obtained in Ref. [64] for general partial waves using the wave function in the cutoff model. It is shown in Ref. [65] that the compositeness of a resonance can be rigorously defined from the wave function with general separable potentials. In Ref. [57], they show that a rank 1 projection operator can be extracted from the residues of the pole of a resonance and suggest the quantity that can be interpreted as a probability of compositeness. In Ref. [66], it is shown that the compositeness extended to a resonance state in a finite volume system can be interpreted as the probability.

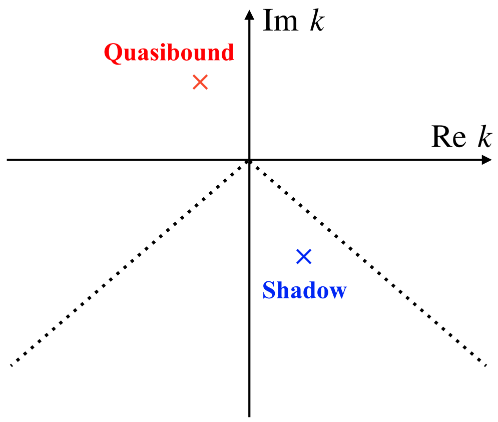

Figure 1.6: The positions of the eigenstate pole and its shadow pole in the k_2-plane. The sign of the imaginary part of the eigen-momentum channel 1 is minus; $\mathrm{Im}\, k_1 < 0$. Thus the upper half and lower half of the k_2-plane correspond to the (2,1) sheet and the (2,2) sheet of the energy plane, respectively.

1.2.4 Pole counting rule

The pole counting rule, which utilizes a relation between the origin of the eigenstate and the pole structure of the scattering amplitude, is proposed in Refs. [67, 68] to study the nature of the $f_0(980)$ meson from the $K\bar{K}$ scattering amplitude. With this rule, we can qualitatively distinguish whether the origin of the eigenstate is the dynamics of the scattering channel of the interest or the hidden channel.

The pole counting rule is derived from the fact that the magnitude of the effective range r_0 is bounded above by the range of the interaction R_{range} as $|r_0| \lesssim R_{\text{range}}$ if the eigenstate is originated in the interaction of the scattering channel of interest. Let us consider the single channel problem.[12] For the near-threshold eigenstate, the positions of two poles in this energy region are given by Eq. (1.2.3). In this case, the distance of the poles in the complex k-plane is given as

$$\left| k_{\text{pole},-} - k_{\text{pole},+} \right| = \left| \frac{2}{r_0} \sqrt{1 + \frac{r_0}{a_0}} \right| \gtrsim \frac{1}{R_{\text{range}}}. \tag{1.2.8}$$

[12]The following discussion can be also applied to the single channel problem with complex threshold parameters where decay channels are already traced out.

For the short range interaction, this distance must be large (e.g. the distance is $\gtrsim 100$ MeV for $R_{\text{range}} \sim 2$ fm). If the eigenstate pole lies in the near-threshold region, the other pole cannot lie in this region. Thus, only one pole can lie in the near-threshold energy region. On the other hand, if the origin is not in the scattering channel of interest, the effective range r_0 is not bounded and can be large (e.g. for the case where a CDD zero lies close to the threshold energy). In this case, the energy difference between the poles can be small and the two poles may lie in the near-threshold region. The position of the poles satisfies that $k_{\text{pole},-} \sim -k_{\text{pole},+}$ because the second term in rhs of Eq. (1.2.3) is dominant. Thus, depending on the origin of the eigenstate, the number of the poles in the near-threshold energy region is different. The pole lying in the Riemann sheet different from the relevant Riemann sheet where the pole representing the physical eigenstate lies is called shadow pole [69].

Let us consider the two-channel problem where the threshold energies $E_{\text{th},i}$ satisfy $E_{\text{th},1} < E_{\text{th},2}$. Suppose that an eigenstate, which originates in the channel $i = 1$, emerges just below the threshold energy of channel 2. The pole representing eigenstate E_{pole} lies in the (2,1) sheet.[13] Applying the above discussion to the eigen-momentum of channel 2, the shadow pole $E_{\text{shadow}}(\sim E_{\text{pole}})$ emerges in the (2,2) sheet (See Fig. 1.6). As in the case of single channel problem, the positions of the eigenstate pole and shadow pole satisfy that $k_{\text{pole},-} \sim -k_{\text{pole},+}$.

The pole counting rule utilizes the above relation between the origin of the eigenstate and the position of the poles to discuss the structure of the eigenstate. The statement of the pole counting rule can be simply summarized as follows;

- If a shadow pole emerges, the origin of the eigenstate is in the hidden channel;
- If a shadow pole does not emerge, the origin of the eigenstate is in the channel of interest.

By "counting" the number of the poles in the near-threshold region, the origin of the eigenstate can be qualitatively distinguished. Note that the pole counting rule can be applied only for the s wave-state.

The statement of the pole counting is related to the compositeness [61]. Let us consider the origin of the s-wave stable weak-binding state. Among the poles of Eq. (1.2.3),

[13] We employed the same notation of the Riemann sheets as in Sect. 1.2.1.

$k_{\text{pole},+}$ represents the bound state and is related to the binding energy as $k_{\text{pole},+} = i\sqrt{2\mu E_B}$ with the reduced mass μ. Then, utilizing weak binding relations, the antibound pole $k_{\text{pole},-}$ can be written with the compositeness X as

$$k_{\text{pole},-} = -i\sqrt{2\mu E_B}\frac{1+X}{1-X} \tag{1.2.9}$$

When the eigenstate is purely composite state $X \sim 1$, $k_{\text{pole},-}$ must lie far from the threshold region and the number of the poles in this region is one. However, when the eigenstate has the hidden channel origin $X \sim 0$, the antibound pole satisfies $|k_{\text{pole},-}| \sim |k_{\text{pole},+}|$, which means that the both the bound state pole and antibound pole lie close to the threshold energy region. Thus for the case where the weak-binding relation works well, the pole counting rule also works well.

While we can quantitatively discuss through the compositeness determined by the weak-binding, the pole counting rule only gives us the qualitative result. However, the pole counting has the broader applicability because the pole counting rule can be directly applied to the near-threshold resonance state.

1.3 Purpose of this work

With the recent development of the experiments, various hadron states are detected and their characteristics are being revealed. Among them, one of the most significant achievements is the discovery of the many candidates of the exotic hadron states, which were theoretically predicted in the early stage of the hadron spectroscopy but were hard to find. Motivated by this progress, to identify the exotic hadron states is the urgent task of the hadron physics. This is because the information about the favored quark-configuration for the hadron internal structure will give us a clue to the understand the low-energy QCD.

To identify a candidate of the exotics, we have to consider the various possible structures that are consistent with its quantum numbers. However, it is very difficult to distinguish which model description is the most appropriate to describe the internal structure of hadrons because of the model dependence. To avoid the theoretical uncertainty, we need to discuss structure based on the quantities that can be uniquely determined from the experimental observables. As such quantities, the on-shell scattering amplitude of the two-body scattering is the fundamental physical quantity which has the abundant information on the eigenstate, e.g. the position of pole, the residue of the pole, or the position of the CDD zero. Thus, by deriving the relation between the on-shell scattering amplitude and the structure of the eigenstate, we can develop the method to investigate the exotic hadron candidates without model dependence. As methods of investigating the structure of the eigenstates from the scattering amplitude, we have seen the two methods; one is the method utilizing the weak-binding relation to evaluate the compositeness and the other is the pole counting rule.

With the former one, we can quantitatively discuss the structure of eigenstates thanks to the probabilistic interpretation for the compositeness. However, we cannot apply this method to the candidates of the exotic hadrons because there is no direct extension of the weak-binding relation for the unstable state and most of the candidates are unstable due to the decay modes. Furthermore, to apply the weak-binding relation, we need the assumption that the effective range expansion works well to describe the eigenstate. However, this assumption does not always hold, e.g. the case where a nearby CDD zero lies close to the eigenstate pole. Thus, it is also important to discuss the extension of the weak-binding relation for such cases.

With the pole counting rule, the origin of the eigenstate can be qualitatively distinguished from the number of the poles in the complex energy plane. Compared to the method utilizing the weak-binding relation, this method has the broader applicability including the unstable states. However, to apply this method, we have to know the position of the shadow pole which lies in the different Riemann sheet than the one adjacent to the physical energy region. This requires the precise determination of the on-shell scattering amplitude from experimental observables.

The purpose of this work is to distinguish the internal structure of the exotic hadron candidates in a model-independent manner. To this end, discussing the relation between the internal structure of the eigenstate and on-shell scattering amplitude, we have to settle the difficulties of the method utilizing the weak-binding relation and the pole counting rule. In this thesis, we develop the two different methods to distinguish the structure of the candidates of the exotic hadrons.. One method is developed by extending the weak-binding relation to the general cases to ease the conditions. The other method is developed from the discussion of the position of the CDD zero.

In Chapter 2, we extend the weak-binding relation to the general cases. As a first step, we show the derivation of the original weak-binding relation within the nonrelativistic effective field theory. Evaluating the contribution from the decay channel, we obtain the generalized relation for unstable quasibound states. With the extended weak-binding relations, we develop a method to systematically evaluate the error which arises from the correction term of the relation. Finally, we generalize the relation to include the nearby CDD zero contribution with the help of the Padé approximant for the inverse amplitude.

In Chapter 3, we discuss the relation between the analytic structure of the scattering amplitude and the origin of an eigenstate. We introduce the zero coupling limit of the coupled-channel amplitude and we show that the origin of the eigenstate is distinguished from the behavior of the pole in this limit. Based on the topological nature of the phase of the scattering amplitude, it is shown that the pole must encounter with the CDD zero in this limit if the eigenstate has the hidden channel origin. With nonrelativistic field theories, we show that such CDD zero lies close to the pole with the finite coupling. We demonstrate that this relation between the origin of the eigenstate and the positions of the poles and zeros can be utilized to discuss the structure of the hadrons.

In Chapter 4, we apply our methods to various hadrons. As a first step, we revisit the compositeness of the deuteron and we check how the error analysis of the estimation of the compositeness works for this state. After that, with the extended weak-binding relations, we discuss the compositeness of $\Lambda(1405)$, $a_0(980)$, $f_0(980)$, and $N\Omega$ dibaryon. For $\Lambda(1405)$, we also numerically investigate the CDD zero contributino to the $\bar{K}N$ compositeness. In the latter part, we discuss the origin the high-mass pole and low-mass pole of $\Lambda(1405)$ from the position of the poles and CDD zeros.

Chapter 2

Compositeness of the weak-binding state

In this chapter, we discuss the extension of the weak-binding relation, aiming at its application to the actual hadrons. Before discussing the extension of the relation, we first discuss the derivation of the original weak-binding relation based on the nonrelativistic effective field theory in Sect. 2.1. After that, we extend the relation to the unstable state and discuss the prescription to interpret the complex value of the compositeness in Sect. 2.2. We also discuss the extension to the case where the effective range expansion does not work well in Sect. 2.3. Finally, we summarize the discussion of this chapter in Sect. 2.4.

2.1 Derivation of the weak-binding relation based on EFT

2.1.1 Effective field theory

From now on, we aim to derive the original weak-binding relation for the stable bound state based on the nonrelativistic effective field theory. We consider the s-wave scattering of two hadrons, where the bound state emerges near the threshold energy. We assume that the hadrons interact through the short range force with the typical range scale R_{typ}.

Now we introduce the fields ψ and ϕ that correspond to the hadrons in the scattering channel. We also introduce the field B_0 whose quantum numbers are equal to those of the bound state.

The Hamiltonian of the nonrelativistic effective field theory [70, 71] for this system is given as

$$H = H_{\text{free}} + H_{\text{int}} = \int d^3\boldsymbol{x} (\mathscr{H}_{\text{free}} + \mathscr{H}_{\text{int}}), \tag{2.1.1}$$

$$\begin{aligned}\mathscr{H}_{\text{free}} = &\frac{1}{2M}\nabla\psi^\dagger(\boldsymbol{x})\cdot\nabla\psi(\boldsymbol{x}) + \frac{1}{2m}\nabla\phi^\dagger(\boldsymbol{x})\cdot\nabla\phi(\boldsymbol{x}) \\ &+ \frac{1}{2M_0}\nabla B_0^\dagger(\boldsymbol{x})\cdot\nabla B_0(\boldsymbol{x}) + \omega_0 B_0^\dagger(\boldsymbol{x})B_0(\boldsymbol{x}),\end{aligned} \tag{2.1.2}$$

$$\mathscr{H}_{\text{int}} = g_0\left(B_0^\dagger(\boldsymbol{x})\psi(\boldsymbol{x})\phi(\boldsymbol{x}) + \phi^\dagger(\boldsymbol{x})\psi^\dagger(\boldsymbol{x})B_0(\boldsymbol{x})\right) + v_0\psi^\dagger(\boldsymbol{x})\phi^\dagger(\boldsymbol{x})\phi(\boldsymbol{x})\psi(\boldsymbol{x}), \tag{2.1.3}$$

where $\hbar = 1$. This Hamiltonian includes only contact terms in the interaction part. This is because the details of the short range interaction becomes irrelevant when we consider the low energy region only. The ultraviolet divergence of the momentum integration caused by this contact interaction is regularized with the sharp momentum cutoff Λ, that is related to the range of the interaction R_{typ} as $\Lambda \sim 1/R_{\text{typ}}$.

Here we define the scattering state $|\boldsymbol{p}\rangle$ with the relative momentum $\boldsymbol{p}$ and the discrete state $|B_0\rangle$;

$$|\boldsymbol{p}\rangle \equiv \frac{1}{\sqrt{V_p}}\tilde{\psi}^\dagger(\boldsymbol{p})\tilde{\phi}^\dagger(-\boldsymbol{p})|0\rangle, \quad |B_0\rangle \equiv \frac{1}{\sqrt{V_p}}\tilde{B}_0^\dagger(\boldsymbol{0})|0\rangle, \tag{2.1.4}$$

with the vacuum defined as

$$\tilde{\psi}(\boldsymbol{p})|0\rangle = \tilde{\phi}(\boldsymbol{p})|0\rangle = \tilde{B}_0(\boldsymbol{p})|0\rangle = 0 \quad (\text{for } \forall\boldsymbol{p}), \quad \langle 0|0\rangle = 1, \tag{2.1.5}$$

where $\tilde{\alpha}(\boldsymbol{p})$ denotes the Fourier transformation of the operator $\alpha(\boldsymbol{x})$ and $V_p = (2\pi)^3\delta(\boldsymbol{0})$ is the phase space of the system. These states constitute an orthonormal basis of the system; $\langle\boldsymbol{p}|\boldsymbol{p}'\rangle = (2\pi)^3\delta(\boldsymbol{p}-\boldsymbol{p}')$, $\langle B_0|B_0\rangle = 1$ and $\langle\boldsymbol{p}|B_0\rangle = 0$. These states are the eigenstates of the free Hamiltonian (2.1.1) as

$$H_{\text{free}}|\boldsymbol{p}\rangle = \frac{\boldsymbol{p}^2}{2\mu}|\boldsymbol{p}\rangle, \quad H_{\text{free}}|B_0\rangle = \omega_0|B_0\rangle, \tag{2.1.6}$$

with the reduced mass $\mu = Mm/(M+m)$. Because of the phase symmetry of the Hamiltonian (2.1.1), the sum of the number of the particle $\psi(\phi)$ and B_0 is conserved. This conservation law implies that the completeness relation of this sector can be written as

$$\int \frac{d^3\boldsymbol{p}}{(2\pi)^3}|\boldsymbol{p}\rangle\langle\boldsymbol{p}| + |B_0\rangle\langle B_0| = 1. \tag{2.1.7}$$

The model space of our EFT is equivalent to that used in Refs. [60, 65]. Compared to these studies, the advantages of utilizing the EFT is that (i) the definition of the field B_0 is clear, (ii) the completeness relation follows from the particle number conservation law and (iii) the separable interaction is naturally introduced to describe the low energy s-wave interaction.

2.1.2 Definition of the compositeness

Next we define the compoositeness of the bound state within our EFT. We write the bound state as $|\Psi\rangle$, that satisfy the Schrödinger equation as

$$H|\Psi\rangle = E_h|\Psi\rangle, \tag{2.1.8}$$

where $E_h < 0$ is the eigenenergy. Due to the completeness relation (2.1.7), the bound state can be written as the superposition of $|\boldsymbol{p}\rangle$ and $|B_0\rangle$:

$$|\Psi\rangle = \int \frac{d^3\boldsymbol{p}}{(2\pi)^3}\chi(\boldsymbol{p})|\boldsymbol{p}\rangle + c|B_0\rangle, \tag{2.1.9}$$

with the wave function of scattering state $\chi(\boldsymbol{p}) = \langle \boldsymbol{p}|\Psi\rangle$ and the weight of the bare state $c = \langle B_0|\Psi\rangle$.

In order to normalize the bound state, we impose the condition

$$\langle\Psi|\Psi\rangle = 1. \tag{2.1.10}$$

Now the compositeness X (elementariness Z) is defined as the sum of the projections to the scattering state (the projection to the discrete state) in this normalization:

$$X \equiv \int \frac{d^3\boldsymbol{p}}{(2\pi)^3}\langle\Psi|\boldsymbol{p}\rangle\langle\boldsymbol{p}|\Psi\rangle = \int \frac{d^3\boldsymbol{p}}{(2\pi)^3}|\chi(\boldsymbol{p})|^2, \tag{2.1.11}$$

$$Z \equiv \langle\Psi|B_0\rangle\langle B_0|\Psi\rangle = |c|^2. \tag{2.1.12}$$

Due to the normalization condition (2.1.10), these quantities satisfy the sum rule:

$$X + Z = 1. \tag{2.1.13}$$

Because X and Z are non-negative, these values has the upper and lower boundaries as

$$X, Z \in [0, 1]. \tag{2.1.14}$$

These two relations (2.1.13) and (2.1.14) are of great importance because they ensure the probabilistic interpretation of X and Z. Thanks to these we can interpret $X(Z)$ as the probability of finding the scattering (the discrete state) in the bound state $|\Psi\rangle$.

2.1.3 Compositeness and scattering amplitude

By integrating out the degree of the discrete state, the scattering problem of this system reduces to the single channel problem with the effective Hamiltonian:

$$H_{\text{eff}}(E) = H_0 + V(E) \tag{2.1.15}$$

$$H_0 = \int \frac{d^3\boldsymbol{p}}{(2\pi)^3}\left[\frac{\boldsymbol{p}^2}{2M}\tilde{\psi}^\dagger(\boldsymbol{p})\tilde{\psi}(\boldsymbol{p}) + \frac{\boldsymbol{p}^2}{2m}\tilde{\phi}^\dagger(\boldsymbol{p})\tilde{\phi}(\boldsymbol{p})\right], \tag{2.1.16}$$

$$V(E) = \int \prod_{i=1}^{4} \frac{d^3\boldsymbol{p}_i}{(2\pi)^3}(2\pi)^3\delta^3(\boldsymbol{p}_1+\boldsymbol{p}_2-\boldsymbol{p}_3-\boldsymbol{p}_4)v(E)\tilde{\psi}^\dagger(\boldsymbol{p}_1)\tilde{\phi}^\dagger(\boldsymbol{p}_2)\tilde{\phi}(\boldsymbol{p}_3)\tilde{\psi}(\boldsymbol{p}_4). \tag{2.1.17}$$

Because the effective interaction (2.1.17) takes the form of separable type, the Lippmann-Schwinger equation for the on-shell T matrix $t(E)$ can be written as

$$t(E) = v(E) + v(E)G(E)t(E), \tag{2.1.18}$$

$$G(E) \equiv \int \frac{d^3\boldsymbol{p}}{(2\pi)^3}\frac{1}{E - p^2/(2\mu) + i0^+}, \tag{2.1.19}$$

$$v(E) = \langle \boldsymbol{p}'|V(E)|\boldsymbol{p}\rangle = v_0 + \frac{g_0^2}{E-\omega_0}, \tag{2.1.20}$$

where $G(E)$ is the loop function of the field ψ and ϕ and $v(E)$ is the effective interaction which includes the contribution from the coupling with the discrete state B_0. We regularize the ultraviolet divergence of the integral in $G(E)$ with the cutoff Λ. By solving the scattering equation algebraically, we obtain the solution for $t(E)$ and the scattering amplitude $\mathscr{F}(E) = -(\mu/2\pi)t(E)$ as

$$t(E) = \frac{1}{[v(E)]^{-1} - G(E)}, \quad \mathscr{F}(E) = -\frac{\mu}{2\pi}\frac{1}{[v(E)]^{-1} - G(E)}. \tag{2.1.21}$$

Since no approximation has been introduced, this is the exact solution of the two-body scattering problem in this EFT.

Let us express the compositeness (2.1.11) within the terms of the scattering problem. Using the Schrödinger equation, we obtain following expression

$$\begin{aligned}\frac{X}{Z} &= -\left(\frac{v_0}{g_0}(E_h-\omega_0)+g_0\right)^2\int\frac{d^3\boldsymbol{p}}{(2\pi)^3}\frac{1}{[(E_h-p^2/(2\mu)^2)]^2}\\ &= -[v^2(E_h)/v'(E_h)]G'(E_h),\end{aligned} \tag{2.1.22}$$

where $A'(E)$ denote the energy derivative of a function $A(E)$. With the sum rule (2.1.13), the compositeness can be written as

$$\begin{aligned}X &= \frac{G'(E_h)}{G'(E_h)-[1/v(E_h)]'}\\ &= -g^2G'(E_h),\end{aligned} \tag{2.1.23}$$

where g is the coupling constant between the scattering state and the bound state defined from the residue of the bound state pole as

$$g^2 \equiv \lim_{E\to E_h}(E-E_h)t(E), \tag{2.1.24}$$

$$\begin{aligned}&= \lim_{E\to E_h}\frac{E-E_h}{v^{-1}(E)-G(E)}\\ &=\frac{1}{[1/v(E_h)]'-G'(E_h)}.\end{aligned} \tag{2.1.25}$$

Now let us discuss the feature of the compositeness. From Eq. (2.1.23), we see that if the coupling between the scattering state and the discrete state is switched off ($g_0 = 0$) and the effective interaction $v(E)$ has no energy dependence, the compositeness must be equal to unity. This means that the energy dependence of the interaction of Eq. (2.1.20), introduced through the coupling to the discrete state in our EFT, causes the deviation of the value of the compositeness from unity. If we introduce a coupling to another channel or another discrete state, its contribution only appears as the energy dependence of the interaction. In our EFT, all contribution of the hidden channels is represented by the discrete channel B_0.

Let us also consider the cutoff dependence of the compositeness. The compositeness is cutoff dependent quantity because the wave function $\chi(\boldsymbol{p})$, utilized in the definition of the compositeness (2.1.11), is not an observable and is in general cutoff dependent quantity. In Eq. (2.1.23), the cutoff dependence of the compositeness is included only in the $G'(E_h)$ while g^2 is the cutoff independent. This is because g^2 is defined from the scattering amplitude with Eq. (2.1.24), which is the observables.

2.1.4 Weak-binding relation

Next assuming the binding energy $-E_h$ is small, we express the compositeness only with the experimental observables and we derive the weak-binding relation. There are two ways to derive this relation. One way is to directly express the coupling constant with the threshold quantities of the amplitude. The other way is to expand the inverse of the scattering length. We show the both derivation in the following.

In the first method, we evaluate the two factors in Eq. (2.1.23) separately. Let us first consider to expand the derivative of the loop function. By performing the integral, the loop function is expressed as

$$G(E) = \frac{\mu}{\pi^2}\left[-\Lambda + \sqrt{2\mu E}\ \mathrm{arctanh}\left(\frac{\Lambda}{\sqrt{2\mu E}}\right)\right] \tag{2.1.26}$$

In the low energy region, we can expand this expression with respect to the energy as

$$G(E) = \frac{\mu}{\pi^2}\left[-\Lambda - \frac{i}{2}\pi\sqrt{2\mu E} + \frac{2\mu E}{\Lambda} + \frac{(2\mu E)^2}{3\Lambda^3} + \cdots\right]. \tag{2.1.27}$$

Then the derivative of the loop function in the low energy region is written as

$$G'(E) = -\frac{i\mu^{3/2}}{\sqrt{8}\pi}\frac{1}{\sqrt{E}} + \frac{2\mu^2}{\pi^2\Lambda} + \frac{8\mu^3 E}{3\pi^2\Lambda^3} + \cdots.$$

Now we assume that the binding energy is small enough to satisfy

$$R_{\mathrm{typ}}/R \ll 1, \quad R \equiv \frac{1}{\sqrt{-2\mu E_h}}, \tag{2.1.28}$$

where R denotes the radius of the wave function. Then $G'(E_h)$ can be obtained as

$$G'(E_h) = -\frac{\mu^2 R}{2\pi}\left\{1 + \mathscr{O}\left(\frac{R_{\mathrm{typ}}}{R}\right)\right\}, \tag{2.1.29}$$

where we have used $\Lambda = 1/R_{\mathrm{typ}}$. Now we can see that the leading term of the expansion in Eq.(2.1.29) is expressed only with the eigenenergy while the higher-order terms include the cutoff.

Next we consider the evaluation of the coupling constant g (or the residue of the pole g^2) with the physical observables. Now we introduce the effective range expansion for the s-wave scattering amplitude:

$$f(p) = \frac{1}{-\frac{1}{a_0} - ip + \frac{r_e}{2}p^2 + \mathscr{O}(R_{\text{eff}}^3 p^4)}, \tag{2.1.30}$$

where $R_{\text{eff}} \sim 1/\Lambda$ denotes the length scale characterizing this expansion and $\mathscr{O}(R_{\text{eff}}/R)$ denotes the higher-order terms. Then we require that the bound state can be well described with this amplitude. This requirement means that the eigenenergy can be well approximated by the threshold parameters and the higher-order terms of the effective range expansion has the negligible contribution as

$$-\frac{R}{a_0} + 1 - \frac{r_e}{2R} + \mathscr{O}\left(\left(\frac{R_{\text{eff}}}{R}\right)^3\right) = 0, \quad \left(\frac{R_{\text{eff}}}{R}\right)^3 \ll 1 \tag{2.1.31}$$

Using the effective range expansion, we obtain the following expression of the residue of the pole:

$$\begin{aligned} g^2 &= \frac{2\pi}{\mu^2 R}\frac{1}{1 - r_e/R + \mathscr{O}((R_{\text{eff}}/R)^3)}, \\ &= \frac{2\pi}{\mu^2 R}\frac{1}{2R/a_0 - 1 + \mathscr{O}((R_{\text{eff}}/R)^3)}. \end{aligned} \tag{2.1.32}$$

The second equality follows from Eq. (2.1.31).

By substituting Eqs. (2.1.29) and (2.1.32) into Eq. (2.1.23), we obtain the weak-binding relations:

$$X = \frac{1}{2R/a_0 - 1 + \mathscr{O}\left(\left(\frac{R_{\text{eff}}}{R}\right)^3\right)}\left[1 + \mathscr{O}\left(\frac{R_{\text{typ}}}{R}\right)\right], \tag{2.1.33}$$

$$X = \frac{1}{1 - r_e/R + \mathscr{O}\left(\left(\frac{R_{\text{eff}}}{R}\right)^3\right)}\left[1 + \mathscr{O}\left(\frac{R_{\text{typ}}}{R}\right)\right]. \tag{2.1.34}$$

These can be rewritten as

$$a_0 = R\left\{\frac{2X}{1+X} + \mathscr{O}\left(\frac{R_{\text{typ}}}{R}\right) + \mathscr{O}\left(\left(\frac{R_{\text{eff}}}{R}\right)^3\right)\right\}, \tag{2.1.35}$$

$$r_e = R\left\{\frac{1-X}{X} + \mathscr{O}\left(\frac{R_{\text{typ}}}{R}\right) + \mathscr{O}\left(\left(\frac{R_{\text{eff}}}{R}\right)^3\right)\right\}. \tag{2.1.36}$$

We see that the leading term of the expansion of the scattering length is determined only by the compositeness X. In the weak-binding limit $E_h \to 0$, the higher-order terms of the expansion $\mathscr{O}(R_{\text{typ}}/R)$ and $\mathscr{O}((R_{\text{eff}}/R)^3)$ must be negligible. In this case, the compositeness X can be determined only by the experimental observables a_0 (or r_e) and E_h. When the binding energy is finite but small enough to satisfy the weak-binding conditions Eqs. (2.1.28) and (2.1.31), the higher-order terms just give the small correction to the value of the compositeness.

Now let us remember that the compositeness X is in general a cutoff dependent quantity. In the weak-binding relation (2.1.35), this cutoff dependence of X is canceled out by that of the higher-order terms of $\mathscr{O}(R_{\text{typ}}/R)$ while the all the other terms (a_0, R) are cutoff-independent quantities. This means that, for the weak-binding state, the value of the compositeness is almost determined by the cutoff-independent observables and the cutoff dependent part of compositeness is just small.

To obtain the well known expression [60], one can simplify the relations by assuming $(R_{\text{eff}}/R)^3 \lesssim R_{\text{typ}}/R$ as

$$a_0 = R\left\{\frac{2X}{1+X} + \mathscr{O}\left(\frac{R_{\text{typ}}}{R}\right)\right\}, \tag{2.1.37}$$

$$r_e = R\left\{\frac{1-X}{X} + \mathscr{O}\left(\frac{R_{\text{typ}}}{R}\right)\right\}. \tag{2.1.38}$$

Now let us discuss the other derivation of the weak-binding relation. By expanding the scattering amplitude around $E = E_h$ and substituting $E = 0$, the scattering length can be expressed as

$$\begin{aligned}\frac{1}{a_0} &= -\frac{1}{\mathscr{F}(E=0)} = \frac{2\pi}{\mu}\left[E_h\left(G'(E_h) - [1/v(E_h)]'\right) + \Delta v^{-1} - \Delta G\right] \\ &= \frac{2\pi}{\mu}\left[\frac{E_h G'(E_h)}{X} + \Delta v^{-1} - \Delta G\right],\end{aligned} \tag{2.1.39}$$

$$\Delta v^{-1} \equiv \sum_{n=2}\frac{1}{n!}\left.\frac{d^n v^{-1}}{dE^n}\right|_{E=E_h}(-E_h)^n, \quad \Delta G \equiv \sum_{n=2}\frac{1}{n!}\left.\frac{d^n G}{dE^n}\right|_{E=E_h}(-E_h)^n, \tag{2.1.40}$$

where we have utilized Eq. (2.1.23). We already know that the leading term of $G'(E_h)$ can be expressed only with the binding energy. What we have to do is to estimate the other terms in Eq. (2.1.39). The higher-derivative terms of the loop function ΔG can be easily evaluated using Eq. (2.1.26) as

$$\left.\frac{d^nG}{dE^n}\right|_{E=E_h} = -(2n-3)!!\left(\frac{-1}{2}\right)^{n+1}\frac{i\mu^{3/2}}{\sqrt{2}\pi}E_h^{-(2n-1)/2}\left[1+\mathscr{O}\left(\left(\frac{R_{\mathrm{typ}}}{R}\right)^{2n-1}\right)\right], \tag{2.1.41}$$

$$\begin{aligned}\Delta G &= \sum_{n=2}\frac{1}{n!}\left.\frac{d^nG}{dE^n}\right|_{E=E_h}(-E_h)^n \\ &= \frac{\mu}{2\pi R}\sum_{n=2}\frac{(2n-3)!!}{n!2^n}\left[1+\mathscr{O}\left(\left(\frac{R_{\mathrm{typ}}}{R}\right)^{2n-1}\right)\right] \\ &= \frac{\mu}{4\pi R}\left[1+\mathscr{O}\left(\frac{R_{\mathrm{typ}}}{R}\right)\right].\end{aligned} \tag{2.1.42}$$

In order to estimate the contribution of Δv^{-1}, we assume that the bound state can be well described by the effective range expansion (2.1.30). Because the expansion Δv^{-1} starts from E_h^2, in order for the scattering length (2.1.39) to match this expansion, the order of Δv^{-1} must be estimated as

$$\Delta v^{-1} = \frac{\mu}{R}\mathscr{O}\left(\left(\frac{R_{\mathrm{eff}}}{R}\right)^3\right). \tag{2.1.43}$$

By substituting Eqs. (2.1.29), (2.1.42), and (2.1.43) into expression of the scattering length (2.1.39), we obtain the weak-binding relation (2.1.35). When we consider the extension of the relation for the quasibound state later, this derivation is useful to estimate the contribution of the decay channel.

2.1.5 Error evaluation of compositeness

When we apply the weak-binding relation (2.1.37) to the actual hadrons to estimate the compositeness, the correction which comes from the higher-order terms should be adequately treated. Here we show how to systematically estimate the compositeness from the experimental observables including the error contribution.

By rewriting the weak-binding relation (2.1.37) as

$$X = \frac{a_0/R+\mathscr{O}(R_{\mathrm{typ}}/R)}{2-\left[a_0/R+\mathscr{O}(R_{\mathrm{typ}}/R)\right]}, \tag{2.1.44}$$

we find that the correction term appears in the form of $a_0/R+\mathscr{O}(R_{\mathrm{typ}}/R)$. Because the higher-order terms are model-dependent quantities, we cannot determine the magnitude of the $\mathscr{O}(R_{\text{typ}}/R)$. So we simply assume the magnitude of this term as R_{typ}/R. When one considers the application to the actual hadrons, the typical length of the interaction is determined as $R_{\text{typ}} = 1/m_{\text{typ}}$, where m_{typ} is the mass of the lightest meson that can be exchanged in the hadron-hadron system. In the other cases, e.g. specific model calculations, R_{typ} can be determined by the spatial range of the potential, or by inverse of the cutoff.

Then the upper and lower boundaries of the compositeness are expressed as follows

$$X_{\text{u}} = \frac{a_0/R + \xi}{2 - a_0/R - \xi}, \quad X_{\text{l}} = \frac{a_0/R - \xi}{2 - a_0/R + \xi}, \quad \xi \equiv R_{\text{typ}}/R. \tag{2.1.45}$$

The central value is determined by neglecting correction terms in Eq. (2.1.44) as

$$X_{\text{c}} = \frac{a_0/R}{2 - a_0/R}. \tag{2.1.46}$$

and its uncertainty band is estimated with Eq. (2.1.45).

2.2 Extension for quasibound state

2.2.1 Effective field theory

In this section we consider the extension of the weak-binding relation for the unstable state. We consider the quasibound state, which has the mass between the threshold energy of scattering channel (channel 1) and that of the decay channel (channel 2) and has decay mode to the channel 2. Especially, we consider the near-threshold quasibound state, that lies close to the threshold energy of channel 1, and derive the relation between the compositeness of channel 1 and the threshold parameters of channel 1. We assume that typical range scale of interaction of channel 1 and channel 2 are both shorter than the length scale R_{typ}.

Now we introduce the fields ψ_i and ϕ_i that correspond to the scattering channel i for $i = 1$ and 2. We also introduce the field B_0 whose quantum numbers are equal to those of the quasibound state. The Hamiltonian of the nonrelativistic effective field theory for this system is given as

$$H = H_{\mathrm{free}} + H_{\mathrm{int}} = \int d^3\boldsymbol{x}(\mathscr{H}_{\mathrm{free}} + \mathscr{H}_{\mathrm{int}}), \tag{2.2.1}$$

$$\begin{aligned}\mathscr{H}_{\mathrm{free}} = \sum_{i=1,2}\left[\frac{1}{2M_i}\nabla\psi_i^\dagger(\boldsymbol{x})\cdot\nabla\psi_i(\boldsymbol{x}) + \frac{1}{2m_i}\nabla\phi_i^\dagger(\boldsymbol{x})\cdot\nabla\phi_i(\boldsymbol{x})\right] + \frac{1}{2M_0}\nabla B_0^\dagger(\boldsymbol{x})\cdot\nabla B_0(\boldsymbol{x})\\ -\omega_\psi\psi_2^\dagger(\boldsymbol{x})\psi_2(\boldsymbol{x}) - \omega_\phi\phi_2^\dagger(\boldsymbol{x})\phi_2(\boldsymbol{x}) + \omega_0 B_0^\dagger(\boldsymbol{x})B_0(\boldsymbol{x}).\end{aligned} \tag{2.2.2}$$

$$\begin{aligned}\mathscr{H}_{\mathrm{int}} = \sum_{i=1,2} g_{0,i}\left(B_0^\dagger(\boldsymbol{x})\psi_i(\boldsymbol{x})\phi_i(\boldsymbol{x}) + \phi_i^\dagger(\boldsymbol{x})\psi_i^\dagger(\boldsymbol{x})B_0(\boldsymbol{x})\right)\\ + \sum_{i,j=1,2} v_{0,ij}\psi_j^\dagger(\boldsymbol{x})\phi_j^\dagger(\boldsymbol{x})\phi_i(\boldsymbol{x})\psi_i(\boldsymbol{x}),\end{aligned} \tag{2.2.3}$$

where $g_{0,i}$ and $v_{0,ij}$ are the coupling constants of three- and four-point interactions, respectively. The ultraviolet divergence of the momentum integral is tamed with the momentum cutoff $\Lambda \sim 1/R_{\mathrm{typ}}$.

We define the eigenstates of the free Hamiltonian as

$$|\boldsymbol{p}_i\rangle \equiv \frac{1}{\sqrt{V_p}}\tilde{\psi}_i^\dagger(\boldsymbol{p})\tilde{\phi}_i^\dagger(-\boldsymbol{p})|0\rangle \quad (i = 1, 2), \tag{2.2.4}$$

$$|B_0\rangle \equiv \frac{1}{\sqrt{V_p}}\tilde{B}_0^\dagger(\boldsymbol{0})|0\rangle, \tag{2.2.5}$$

where the vacuum is defined in the same way as in Eq. (2.1.5). These states are normalized and orthogonal to each other. The eigenenergy of these states are $\boldsymbol{p}^2/(2\mu_i) - \omega\delta_{i,2}$ and ω_0, where $\mu_i = M_i m_i/(M_i + m_i)$ is the reduced mass of channel i and $\omega = \omega_\psi + \omega_\phi$ is the difference between the threshold energy of channel 1 and 2. Because of the conservation law, the completeness relation of the sector of interest is written with the above eigenstates as

$$\sum_{i=1,2} \int \frac{d^3\boldsymbol{p}}{(2\pi)^3} |\boldsymbol{p}_i\rangle\langle\boldsymbol{p}_i| + |B_0\rangle\langle B_0| = 1. \tag{2.2.6}$$

2.2.2 Definition of compositeness

Now we assume that the system has the quasibound state $|\Psi_{\mathrm{QB}}\rangle$ with complex eigenenergy E_h, that satisfies the Schrödinger equation as

$$H|\Psi_{\mathrm{QB}}\rangle = E_h|\Psi_{\mathrm{QB}}\rangle, \tag{2.2.7}$$

$$|\Psi_{\mathrm{QB}}\rangle = \sum_{i=1,2} \int \frac{d^3\boldsymbol{p}}{(2\pi)^3} \chi_i(\boldsymbol{p})|\boldsymbol{p}_i\rangle + c|B_0\rangle, \tag{2.2.8}$$

where $\chi_i(\boldsymbol{p})$ and c denote the wave function. In order to define the compositeness with the projection operators, we have to normalize the eigenstate. However the standard normalization condition used for the bound state (2.1.10) is not applicable for the unstable state. Instead, we employ the Gamow normalization, which utilizes the Gamow state of the eigenstate:

$$|\tilde{\Psi}_{\mathrm{QB}}\rangle \equiv \sum_{i=1,2} \int \frac{d^3\boldsymbol{p}}{(2\pi)^3} \chi_i^*(\boldsymbol{p})|\boldsymbol{p}_i\rangle + c^*|B_0\rangle. \tag{2.2.9}$$

The Gamow normalization condition is given by

$$\langle\tilde{\Psi}_{\mathrm{QB}}|\Psi_{\mathrm{QB}}\rangle = \sum_{i=1,2} \int \frac{d^3\boldsymbol{p}}{(2\pi)^3} \chi_i^2(\boldsymbol{p}) + c^2 = 1. \tag{2.2.10}$$

Then, using the projection operators, we can define the compositeness of the compositeness of channel i and elementariness Z as

$$X_i \equiv \int \frac{d^3\boldsymbol{p}}{(2\pi)^3} \langle\tilde{\Psi}_{\mathrm{QB}}|\boldsymbol{p}_i\rangle\langle\boldsymbol{p}_i|\Psi_{\mathrm{QB}}\rangle = \int \frac{d^3\boldsymbol{p}}{(2\pi)^3} \chi_i^2(\boldsymbol{p}), \quad Z \equiv \langle\tilde{\Psi}_{\mathrm{QB}}|B_0\rangle\langle B_0|\Psi_{\mathrm{QB}}\rangle = c^2. \tag{2.2.11}$$

Note that X_i and Z are all complex numbers due to the unstable nature of the eigenstate. With the normalization condition (2.2.10) and the completeness relation (2.2.6), the sum rule for X_i and Z is found to be

$$X_1 + X_2 + Z = 1. \tag{2.2.12}$$

For the bound sate, the values of the compositeness and elementariness are bounded with Eq. (2.1.14). However, there is no corresponding condition for the real part or imaginary part of X_i of the quasibound state . Due to the lack of this condition and the complex value of the compositeness, we cannot consider X_i as the probabilities. To interpret these complex values, we need a prescription, that we will discuss in Sect. 2.2.5.

2.2.3 Compositeness and scattering amplitude

From now on, we derive the elastic scattering amplitude of channel 1 $t(E)$. As in Sect. 2.1, we can derive the effective single-channel Lippmann-Schwinger equation for channel 1 as

$$t(E) = v_1^{\text{eff}}(E) + v_1^{\text{eff}}(E)G_1(E)t(E), \tag{2.2.13}$$

where v_1^{eff} is the effective interaction for channel 1 including the contribution of the scattering channel 2 and discrete channel given as

$$v_1^{\text{eff}}(E) \equiv v_{11}(E) + \frac{v_{12}^2(E)}{[G_2(E)]^{-1} - v_{22}(E)}, \tag{2.2.14}$$

$$v_{ij}(E) \equiv v_{0,ij} + \frac{g_{0,i}g_{0,j}}{E-\omega_0}, \quad G_i(E) \equiv \int \frac{d^3\boldsymbol{p}}{(2\pi)^3} \frac{1}{E - p^2/(2\mu_i) + \delta_{i,2}\omega + i0^+}. \tag{2.2.15}$$

By solving the Lippmann-Schwinger equation, the exact on-shell T matrix and the scattering amplitude of channel 1 is given as

$$t(E) = \frac{1}{[v_1^{\text{eff}}(E)]^{-1} - G_1(E)}, \tag{2.2.16}$$

$$\mathscr{F}(E) = -\frac{\mu_1}{2\pi} \frac{1}{[v_1^{\text{eff}}(E)]^{-1} - G_1(E)}. \tag{2.2.17}$$

Let us consider to express the compositeness (2.2.11) within the terms of the scattering problem. Using the Schrödinger equation, we obtain

$$\chi_i(\boldsymbol{p}) = \frac{1}{E_h - p^2/(2\mu_i) + \delta_{i,2}\omega} \sum_j v_{ij}(E_h)\alpha_j, \tag{2.2.18}$$

$$c = \sum_{i=1,2} \frac{g_{0,i}}{E_h - \omega_0} \alpha_i, \quad \alpha_i \equiv \int \frac{d^3\boldsymbol{p}}{(2\pi)^3} \chi_i(\boldsymbol{p}), \tag{2.2.19}$$

which lead to

$$X_i = -G_i'(E_h)\beta_i^2, \quad Z = -\sum_{i,j} G_i(E_h) v_{ij}'(E_h) G_j(E_h)\beta_i\beta_j, \quad \beta_i \equiv \sum_j v_{ij}(E_h)\alpha_j. \tag{2.2.20}$$

Using these expressions, we obtain the following expression for the compositeness of channel 1:

$$\begin{aligned} X_1 &= \frac{G_1'(E_h)}{G_1'(E_h) - \left[1/v_1^{\mathrm{eff}}(E_h)\right]'} \\ &= -g_1^2 G_1'(E_h), \end{aligned} \tag{2.2.21}$$

where g_1 is the coupling constant between the scattering state and the bound state defined from the residue of the eigenstate pole as

$$g_1^2 \equiv \lim_{E \to E_h} (E - E_h) t(E) = \frac{1}{[1/v_1^{\mathrm{eff}}(E_h)]' - G_1'(E_h)}. \tag{2.2.22}$$

Note that the expression for the compositeness (2.2.21) is obtained by replacing $G \to G_1$ and $v \to v_1^{\mathrm{eff}}$ in Eq. (2.1.23). The expression of the compositeness of channel 2 is given as

$$\begin{aligned} X_2 &= \frac{G_2'(E_h)}{G_2'(E_h) - \left[1/v_2^{\mathrm{eff}}(E_h)\right]'} \\ &= -g_2^2 G_2'(E_h) \end{aligned} \tag{2.2.23}$$

$$Z = 1 - X_1 - X_2 \tag{2.2.24}$$

where v_2^{eff} and g_2 are defined by replacing the symbols of channel number as $1 \leftrightarrow 2$ in Eq. (2.2.14) and Eq. (2.2.22), respectively.

2.2.4 Weak-binding relation

Here we derive the weak-binding relation for the quasibound state by assuming the absolute value of the eigenenergy of the quasibound state is small. The simplest way to derive the relation is to express the coupling constant g_1 with the effective range expansion as in the same procedure with the bound state case. On the other hand, by using the expansion of the inverse of the scattering length, the contribution from the decay mode can be estimated.

Let us show the derivation by to expressing the coupling constant with the effective range expansion. First we assume that the absolute value of the eigenenergy is small enough to satisfy

$$\frac{R_{\rm typ}}{|R|} \ll 1, \quad R \equiv \frac{1}{\sqrt{-2\mu_1 E_h}}. \tag{2.2.25}$$

Note that, unlike R for the bound state defined in Eq. (2.1.28), R for the bound state defined here is complex because the eigenenergy is also complex. The expression of the loop function of channel 1 is obtained by replacing $\mu \to \mu_1$ in Eq. (2.1.26). Then the energy derivative of loop function in Eq. (2.2.21) is estimated as

$$G'(E_h) = -\frac{\mu_1^2 R}{2\pi}\left\{1+\mathscr{O}\left(\frac{R_{\rm typ}}{R}\right)\right\}. \tag{2.2.26}$$

As done in the bound state case with Eq. (2.1.31), by assuming the convergence region of the effective range expansion reaches the eigenstate pole;

$$|R_{\rm eff}/R|^3 \ll 1, \tag{2.2.27}$$

the residue of the pole is expressed as

$$g_1^2 = \frac{2\pi}{\mu^2 R}\frac{1}{2R/a_0 - 1 + \mathscr{O}(|R_{\rm eff}/R|^3)}, \tag{2.2.28}$$

where the scattering length a_0 and effective range r_e are complex due to the coupling to the decay channel. Using Eqs. (2.2.21) and (2.2.28), the weak-binding relation for the quasibound state is obtained as

$$a_0 = R\left\{\frac{2X_1}{1+X_1} + \mathscr{O}\left(\left|\frac{R_{\rm typ}}{R}\right|\right) + \mathscr{O}\left(\left|\frac{R_{\rm eff}}{R}\right|^3\right)\right\}. \tag{2.2.29}$$

We see that this extended relation is similar to that for the bound state. The correction terms are again negligible when the absolute value of the eigenenergy is sufficiently small as $|R_{\rm typ}/R| \ll 1$ and $|R_{\rm eff}/R|^3 \ll 1$. In this case, the compositeness X_1 can be directly determined by the scattering length and eigenenergy.

To estimate the order of the contribution from the decay mode, let us consider another derivation of the relation. Expanding the inverse of the scattering length $a_0 = -\mathscr{F}(0)$ by $1/|R|$, we obtain

$$\frac{1}{a_0} = \frac{2\pi}{\mu_1}\left\{\frac{E_h G_1'(E_h)}{X_1} + \Delta\left[v_1^{\rm eff}\right]^{-1} + \Delta G_1\right\}, \tag{2.2.30}$$

where $\Delta[v_1^{\text{eff}}]^{-1}$ and ΔG_1 are the higher-order terms of the expansion of v_1^{eff} and G_1 defined as

$$\Delta\left[v_1^{\text{eff}}\right]^{-1} = \sum_{n=2} \frac{1}{n!} \left.\frac{d^n[v_1^{\text{eff}}]^{-1}}{dE^n}\right|_{E=E_h} (-E_h)^n. \tag{2.2.31}$$

$$\Delta G \equiv \sum_{n=2} \frac{1}{n!} \left.\frac{d^n G}{dE^n}\right|_{E=E_h} (-E_h)^n. \tag{2.2.32}$$

The estimation of the term of ΔG_1 can be obtained in the same way as done in Eq. (2.1.42);

$$\Delta G_1 = \frac{\mu_1}{4\pi R}\left[1 + \mathscr{O}\left(\left|\frac{R_{\text{typ}}}{R}\right|\right)\right]. \tag{2.2.33}$$

Now let us consider the estimation of $\Delta[v_1^{\text{eff}}]^{-1}$. Using Eq. (2.2.14), $[v_1^{\text{eff}}]^{-1}$ is written down as

$$\left[v_1^{\text{eff}}(E)\right]^{-1} = \frac{1 - G_2(E)v_{22}(E)}{(1 - G_2(E)v_{22}(E))\, v_{11}(E) + G_2(E)v_{12}^2(E)}. \tag{2.2.34}$$

Thus its higher-order terms of the expansion $\Delta\left[v_1^{\text{eff}}\right]^{-1}$ includes higher derivatives of $v_{ij}(E)$ or $G_2(E)$. With Eq. (2.2.15), the n-th derivative of $v_{ij}(E)$ is estimated as $|R_{\text{typ}}/R|^n$. In order to estimate the contribution from the higher-order derivative of $G_2(E)$, let us define the length scale related to the difference between the threshold energies of channel 1 and that of channel 2 as

$$l \equiv \frac{1}{\sqrt{2\mu_1\omega}}. \tag{2.2.35}$$

Using this length scale, the higher derivative of $G_2(E)$ is estimated as

$$\begin{aligned} G_2(E) =& \frac{\mu_2}{\pi^2}\left[-\Lambda + \sqrt{2\mu_2(E+\omega)}\,\text{arctanh}\left(\frac{\Lambda}{\sqrt{2\mu_2(E+\omega)}}\right)\right] \\ =& \frac{\mu_2}{\pi^2}\left[-\Lambda - \frac{i\pi}{2}\sqrt{2\mu_2(E+\omega)} + \frac{2\mu_2(E+\omega)}{\Lambda} + \frac{(2\mu_2(E+\omega))^2}{3\Lambda^3} + \cdots\right], \end{aligned} \tag{2.2.36}$$

$$\begin{aligned} E_h^n \frac{d^n G_2}{dE^n}(E_h) =& \frac{\mu_2}{\pi^2}\left[i\pi\frac{(-1)^{n-1}(2n-3)!!}{2^{n+2}}\sqrt{2\mu_2}\frac{E_h^n}{(E_h+\omega)^{(2n-1)/2}} + \frac{(2\mu_2 E_h)^n}{\Lambda^{2n+1}}(1+\cdots)\right] \\ =& \frac{\mu_1}{R}\left[\mathscr{O}\left(\left(\frac{l}{|R|}\right)^{2n-1}\right) + \mathscr{O}\left(\left(\frac{R_{\text{typ}}}{|R|}\right)^{2n-1}\right)\right], \end{aligned} \tag{2.2.37}$$

where we assume $\mu_2/\mu_1 \sim \mathscr{O}(1)$.[1] We see that this expression contains only the higher-order terms of $R_{\rm typ}/R$ or l/R unlike the higher-order terms of channel 1 ΔG_1 whose expression is obtained in Eq. (2.2.33). This is due to the presence of the energy difference ω. Using these expressions, we obtain

$$\Delta\left[v_1^{\rm eff}\right]^{-1} = \sum_{n=0}^{3}\frac{\mu_1}{R}\mathscr{O}\left(\frac{R_{\rm typ}^n l^{3-n}}{|R|^3}\right). \tag{2.2.38}$$

By utilizing the estimation of each term in Eq. (2.2.30), the scattering length is expressed as

$$\begin{aligned} a_0 = &\frac{\mu_1}{2\pi}\left\{\frac{\mu_1}{4\pi X_1 R} + \frac{\mu_1}{4\pi R} + \frac{\mu_1}{R}\mathscr{O}\left(\left|\frac{R_{\rm typ}}{R}\right|\right) + \frac{\mu_1}{R}\left[\mathscr{O}\left(\left|\frac{R_{\rm typ}}{R}\right|^3\right)\right.\right. \\ &\left.\left. + \mathscr{O}\left(\left|\frac{R_{\rm typ}}{R}\right|^2\right)\mathscr{O}\left(\left|\frac{l}{R}\right|\right) + \mathscr{O}\left(\left|\frac{R_{\rm typ}}{R}\right|\right)\mathscr{O}\left(\left|\frac{l}{R}\right|^2\right) + \mathscr{O}\left(\left|\frac{l}{R}\right|^3\right)\right]\right\}^{-1} \\ = &R\left\{\frac{2X_1}{1+X_1} + \mathscr{O}\left(\left|\frac{R_{\rm typ}}{R}\right|\right) + \mathscr{O}\left(\left|\frac{l}{R}\right|^3\right)\right\}. \end{aligned} \tag{2.2.39}$$

In this expression of the weak-binding relation, we find that the contribution from the decay channel is expressed by the third term. This term can be neglected when the absolute value of the eigenenergy is sufficiently smaller than the difference of the threshold energy ν to satisfy $|l| \ll |R|^3$. In this case, the compositeness X_1 of the quasibound state can be model-independently determined only by the observables.

By performing the same procedure, the relation between the compositeness of channel 2 X_2, the scattering length of channel 2 $a_{0,2}$ and the eigenenergy measured from the threshold energy of channel 2 $E_{h,2}$ can be obtained as

$$a_{0,2} = R_2\left\{\frac{2X_2}{1+X_2} + \mathscr{O}\left(\left|\frac{R_{\rm typ}}{R_2}\right|\right) + \mathscr{O}\left(\left|\frac{l_2}{R_2}\right|^3\right)\right\}, \tag{2.2.40}$$

with $R_2 = 1/\sqrt{-2\mu_2 E_{h,2}}$ and $l_2 = 1/\sqrt{2\mu_2\omega}$. If R_2 satisfies $|R_{\rm typ}/R_2| \ll 1$ and $|l_2/R_2|^3 \ll 1$, X_2 can be also determined from the observables. However, when the eigenstate lies close to the threshold energy of channel 1, these two conditions for R_2 cannot be satisfied

[1]From the concept of EFT, this assumption that there is no specific scale that causes an order difference in the parameters is natural.

simultaneously. For example, if the eigenstate lies close to the threshold energy of channel 2 and satisfy $E_{h,2}$, the difference of the threshold energies must be small and $|l_2/R_2|$ is of the order one. Thus, only the compositeness of the dynamical channel closest to the eigenstate can be determined in a model-independent manner.

2.2.5 Interpretation of complex compositeness

Let us discuss the interpretation of the complex compositeness for unstable states. Though several ways to interpret the complex compositeness has been proposed so far, there is no common or concrete way. Here we consider how we can construct the reasonable prescription to interpret this quantity. From now on, we write $X = X_1$ and $Z = 1 - X_1$ because X_1 (and $1 - X_1$) can be model-independently determined.

By switching off the inter-channel couplings of coupled-channel problem, a quasi-bound state becomes the stable bound state (For detail, see Sect. 3). In this limit, the compositeness X must be real and can be interpreted as a probability. This means that, for the quasibound state with the sufficiently small decay width, the imaginary part of X must be small and its real part must be not greatly exceeds from the region $[0,1]$. In this case, the value of the compositeness X is considered to reflect the amount of the dynamical component. On the other hand, the compositeness for the eigenstate with the large decay width may have the value that cannot be considered to reflect the amount of the dynamical fraction, e.g. $X = 1.8 - i0.1$. In this case, it is not reasonable to discuss the structure from the value of X. The difference between these two cases is the amount of the cancellation in $X + Z = 1$. In the former (later) case, the amount of the cancellation is small (large). Thus it is reasonable to discuss the structure from the calculated compositeness X only when the amount of the cancellation is sufficiently small.

To introduce a prescription to interpret the complex compositeness, firstly we define new real quantities $\tilde{X}$ and $\tilde{Z}$, that are interpreted as the probabilities of finding the composite state and the other state, respectively. In order to consider these quantities as the probabilities, the following conditions must be satisfied:

Condition (1) $\tilde{X}, \tilde{Z} \in [0,1]$;

Condition (2) $\tilde{X} + \tilde{Z} = 1$.

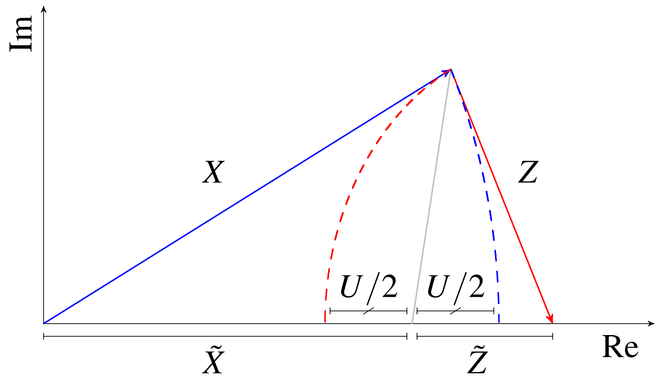

Figure 2.1: Geometric illustration of $\tilde{X}$, $\tilde{Z}$ and U defined in Eq. (2.2.41).

Furthermore, as we have discussed above, in the bound state limit, these probability must be equal to the original definition of X and Z, which are real and interpreted as probabilities. We impose the third condition:

Condition (3) When there is no cancellation in $X+Z$, $\tilde{X}=X$ and $\tilde{Z}=Z$.

Next let us introduce a quantity U which represents the uncertainty of the interpretation. Based on the above discussion, we require U to satisfy:

Condition (4) When there is no cancellation in $X+Z$ then $U=0$;

Condition (5) U increases as the cancellation in $X+Z$ becomes large.

One of the simplest definitions of $\tilde{X}$, $\tilde{Z}$ and U which satisfies all of these conditions is given as

$$\tilde{X} \equiv \frac{1-|Z|+|X|}{2}, \quad \tilde{Z} \equiv \frac{1-|X|+|Z|}{2}, \quad U \equiv |Z|+|X|-1, \tag{2.2.41}$$

whose geometric illustration in the complex plane is drawn in Fig. 2.1. From this figure, one can see that the quantity $\tilde{X}$ is defined by the middle point of $(|X|,0)$ and $(1-|Z|,0)$. The quantity U is defined as deviation of $|X|+|Z|$ from unity. With this definition, $\tilde{X}$ satisfies $|X|-\tilde{X}=U/2$ and $|1-X|-(1-\tilde{X})=U/2$. This implies that the magnitude of the uncertainty of $\tilde{X}$ coming from the complex nature can be regarded as $U/2$ (not U). Only when the uncertainty of the interpretation $U/2$ is small enough, $\tilde{X}$ is considered as the probability with error of $U/2$.

Finally let us discuss the relation between our prescription and those proposed in the previous studies. In Ref. [72], for the application to the multi-channel coupled problem, they define the real-valued compositeness as

$$\tilde{X}' = \frac{|X|}{1+U}, \tag{2.2.42}$$

where U is defined as the same way. Because this definition also satisfies the above conditions(1)-(5), $\tilde{X}$ and $\tilde{X}'$ give the same interpretation when U is sufficiently small. Actually, from the triangle inequalities, we find that

$$|\tilde{X} - \tilde{X}'| \leq \frac{U}{2}, \tag{2.2.43}$$

which means that the difference of these values are small when $U/2$ is small. As other prescriptions, $|X|$ and Re X are proposed to be the probability in Ref. [64] and [73], respectively. The deviation between these values and our $\tilde{X}$ must be again small when $U/2$ is small due to the following relations:

$$\left||X| - \tilde{X}\right| = \frac{U}{2}, \tag{2.2.44}$$

$$\left|\mathrm{Re}\, X - \tilde{X}\right| = \left||X| - |Z|\right|\frac{U}{2} \leq \frac{U}{2}. \tag{2.2.45}$$

However, we note that $|X|$ and Re X are not bounded in $[0,1]$ and these are not always considered as the probabilities.

2.2.6 Error evaluation of compositeness

Let us consider how to evaluate the error of the compositeness coming from the correction terms of the extended weak-binding relation (2.2.29). Since $\tilde{X}$ can be interpreted as the probability, rather than X, we consider the upper and lower boundaries of $\tilde{X}$.

As in the the bound state case in Sect. 2.1, we introduce the quantity ξ_c that expresses the magnitude of the sum of the two correction terms; $\mathscr{O}(|R_{\mathrm{typ}}/R|)$ and $\mathscr{O}(|l/R|^3)$. Because both of them can be complex, the quantity ξ_c can also be complex. We allow ξ_c to vary in the region

$$|\xi_c| \leq |R_{\mathrm{typ}}/R| + |l/R|^3, \tag{2.2.46}$$

where R_{typ} is estimated by the mass of the lightest meson that can be exchanged in the system of the interest and l is determined by the difference of the threshold energy of the scattering channel and that of the channel closest to that scattering channel as in Eq. (2.2.35). While varying ξ_c in the above region, we calculate the compositeness X as

$$X = \frac{a_0/R + \xi_c}{2 - a_0/R - \xi_c}, \tag{2.2.47}$$

and $\tilde{X}$ with Eq. (2.2.41). The upper(lower) boundary $\tilde{X}_{\mathrm{u}}(\tilde{X}_{\mathrm{l}})$ is determined the maximum(minimum) value of $\tilde{X}$ obtained in this procedure. Then we obtain the uncertainty band as $\tilde{X}_{\mathrm{l}} < \tilde{X} < \tilde{X}_{\mathrm{u}}$. The central value $\tilde{X}_{\mathrm{c}}$ is obtained using the value of X calculated with $\xi_c = 0$ in Eq. (2.2.47).

2.3 Extension to include CDD zero contribution

In Sect. 1.2.2, we discussed the importance of including the contribution of nearby CDD (Castillejo–Dalitz–Dyson) zero, which is defined as the zero of the scattering amplitude. However, the weak-binding relation derived above for the bound state or the quasibound state does not include the CDD zero contribution. This is because we have naively assumed that the convergence of the effective range expansion in the above derivation of the weak-binding relation. This point has been already pointed out originally by Weinberg in Ref. [60]. In this section, we extend the weak-binding relation to include the CDD zero contribution. For simplicity, we only consider the case of stable bound state, while the generalization to quasibound state is straightforward.

When the CDD zero E_{CDD} lies close to the threshold energy, the convergence region of the ERE is limited to the small energy region because the ERE amplitude (2.1.30) cannot equals to zero. In this case the ERE may fail to describe the eigenstate pole even if its position is near the threshold. This leads to the large correction term of $\mathscr{O}((R_{\mathrm{eff}}/R)^3)$ in Eq. (2.1.33). Thus the compositeness cannot be determined with the experimental observables with the original weak-binding relation. In Sect. 2.1.4, the ERE is introduced to the estimate the residue of the pole g^2 with the threshold parameters and eigenenergy. To include CDD contribution to the weak-binding relation, we need to improve the way to estimate the residue of the pole.

We note that this failure of the weak-binding relation does not mean the compositeness of the eigenstate accompanied by the nearby CDD zero has the large model-dependent part. The model-dependence or the cutoff dependence is included only in the correction term of $\mathscr{O}(R_{\mathrm{typ}}/R)$ in Eq. (2.1.33), but not in the term of $\mathscr{O}((R_{\mathrm{eff}}/R)^3)$. Thus even if the CDD zero lies close to the threshold, the model-dependent part of the compositeness is still small when the eigenenergy of the state is sufficiently small to satisfy $R_{\mathrm{typ}}/R \ll 1$.

Now let us derive the extended weak-binding relation to include the CDD zero contribution. The s-wave single channel scattering amplitude is written with the phase shift $\delta(p)$ as

$$f(p) = \frac{1}{p\cot\delta - ip}. \tag{2.3.1}$$

The term of $p\cot\delta$ is an analytic function of p^2. By performing Maclaurin expansion for $p\cot\delta$, we obtain the expression of the ERE (2.1.30). To include the CDD zero contribution, we employ the Padé approximant for the expansion of $p\cot\delta$:

$$p\cot\delta = \frac{b_0 + b_1 p^2}{1 + c_1 p^2} + \mathscr{O}\left(R_{\text{Padé}}^5 p^6\right), \tag{2.3.2}$$

where $R_{\text{Padé}}$ is the length scale characterizing this expansion. The position of the CDD zero is expressed as $E_{\text{CDD}} = -1/2\mu c_1$. The relation between the threshold parameters and the expansion coefficients are obtained as

$$a_0 = -\mathscr{F}(0) = -\frac{1}{b_0}, \quad r_{\text{e}} = \left.\frac{d^2\mathscr{F}^{-1}}{dp^2}\right|_{E=0} = 2(b_1 - b_0 c_1). \tag{2.3.3}$$

By substituting Eq. (2.3.2) into Eq. (2.1.24), the residue of the pole g^2 is expressed as

$$g^2 = -\frac{2\pi p}{\mu^2}\left.\left\{\frac{2b_1 p(1 + c_1 p^2) - 2c_1 p(b_0 + b_1 p^2)}{(1 + c_1 p^2)^2} - i + \mathscr{O}\left(R_{\text{Padé}}^5 p^5\right)\right\}^{-1}\right|_{p=i/R}. \tag{2.3.4}$$

With the estimation of the derivative of loop function (2.1.29), the compositeness is written as

$$X = \left[1 - \frac{2(b_1 - c_1 b_0)R^3}{(c_1 - R^2)^2} + \mathscr{O}\left(\left(\frac{R_{\text{Padé}}}{R}\right)^5\right) + \mathscr{O}\left(\frac{R_{\text{typ}}}{R}\right)\right]^{-1}. \tag{2.3.5}$$

Now we see that the compositeness approaches 0 in the limit where the CDD zero approaches to the eigenstate pole $c_1 \to R$. On the other hand, this expression reduces to Eq. (2.1.37) in the case when the CDD zero is infinitely far away from the threshold energy: $c_1 \to 0$. Using the pole condition of amplitude with the Padé expansion (2.3.2):

$$\left(b_0 - b_1\frac{1}{R^2}\right) + \frac{1}{R}\left(1 - c_1\frac{1}{R^2}\right)\left[1 + \mathscr{O}\left(\left(\frac{R_{\text{Padé}}}{R}\right)^5\right)\right] = 0, \tag{2.3.6}$$

we obtain the extended weak-binding relation including the CDD zero contribution expresses with the threshold parameters and the eigenenergy as

$$X = \left[1 - \frac{4R(a_0 - R)^2}{a_0^2 r_{\text{e}}} + \mathscr{O}\left(\left(\frac{R_{\text{Padé}}}{R}\right)^5\right) + \mathscr{O}\left(\frac{R_{\text{typ}}}{R}\right)\right]^{-1}. \tag{2.3.7}$$

With this relation, the compositeness for the weak-binding state can be determined with the threshold parameters and the eigenenergy even when the CDD zero lies close to the eigenstate.

2.4 Summary

In this chapter, we have discussed the extension of the original weak-binding relation to the several cases based on the nonrelativistic effective field theory. Firstly, we have presented the derivation of the weak-binding relation for the bound state within the nonrelativistic effective field theory. With this derivation, it is clarified that the relation is derived with the two independent assumptions, which leads to the two different higher-order terms $\mathscr{O}(R_{\mathrm{typ}}/R)$ and $\mathscr{O}((R_{\mathrm{typ}}/R_{\mathrm{eff}})^3)$. Then analyzing the system including decay channel, the weak-binding relation has been extended for the unstable quasibound state. the compositeness of the near-threshold unstable state is also determined from the complex observables as long as the contribution from the decay mode can be neglected. For the applications to the actual hadrons, we have constructed the prescription to interpret the complex compositeness with the real-valued compositeness $\tilde{X}$ and the uncertainty of the interpretation U. We also constructed the method to estimate errors that arise from the higher-order terms in the weak-binding relation. Finally, by utilizing the Padé approximant, the weak-binding relation is generalized to include the CDD zero contribution. With this extension, it has been shown that the compositeness can be model-independently determined even if the CDD zero lies close to the eigenstate pole. We see the applications of the extended weak-binding relation to the actual hadrons in Sect. 4.

Chapter 3

Structure of the resonance accompanied by a nearby CDD zero

In Chapter 2, the weak-binding relation of the compositeness is extended to the s-wave near-threshold quasibound state. However, this method does not still apply to the hadrons with higher-partial waves or hadrons lying far from the threshold. In order to discuss the structure of such hadrons in a model-independent manner, another method is needed. In this chapter, we derive another relation between the scattering amplitude and structure of resonance state and construct totally new method to discuss the origin of the state.

This chapter is organized as follows. In Sect. 3.1, we introduce the zero coupling limit of the coupled-channel scattering amplitude and argue that the origin of the eigenstate can be distinguished by the behavior of the pole in this limit. In Sect. 3.2, with the discussion of the topological invariant of the scattering amplitude, we show that the origin of the eigenstate can be clarified with is related to the positions of the pole and CDD zero. In Sect. 3.3, we check how the relation works in solvable effective field theories.

3.1 Zero coupling limit of coupled-channel amplitude

The zero coupling limit (ZCL) of the coupled-channel scattering amplitude is defined as the limit of turning off the couplings between different coupled-channels [69, 74–76]. For example, if the coupled-channel system has the interaction $V_{ij}(E)$, its off-diagonal part gives the inter-channel coupling and the ZCL corresponds to the limit of

$$V = \begin{pmatrix} V_{11} & V_{12} & \dots & V_{1N} \\ V_{21} & V_{22} & \dots & V_{2N} \\ \vdots & \vdots & \ddots & \vdots \\ V_{N1} & V_{N2} & \dots & V_{NN} \end{pmatrix} \to \begin{pmatrix} V_{11} & 0 & \dots & 0 \\ 0 & V_{22} & \dots & 0 \\ \vdots & \vdots & \ddots & \vdots \\ 0 & 0 & \dots & V_{NN} \end{pmatrix}. \tag{3.1.1}$$

Let us consider the case where the coupled-channel system has an eigenstate originating in the dynamics of a channel i. In other words, the i-th diagonal component V_{ii} generates an eigenstate by itself. Before taking the ZCL, the pole must exist in the all components of the scattering amplitude. After taking the ZCL, the pole must remain in the amplitude i-th component of the $\mathscr{F}_{ii}$ and must decouple from the other components because V_{ii}, which is the origin of the eigenstate, contributes only to this component of amplitude.[1] If we consider the eigenstate which is purely generated by the coupled-channel effect, its eigenstate pole decouples from the all of the components.

The behavior of the pole in the ZCL discussed above is summarized as follows;

1. If the pole remains in the amplitude $\mathscr{F}_{ii}$ in the ZCL, channel i is the origin of the eigenstate.

2. If the pole decouples from the amplitude $\mathscr{F}_{ii}$ in the ZCL, channel i is not the origin of the eigenstate.

The latter can be divided into two cases. One is the case where the eigenstate originates in another channel j and the pole remains only in the component of the scattering amplitude F_{jj}. The other is the case where the pole decouples from the all of the components. In this case the eigenstate is purely generated by the coupled-channel effect. In both cases, we can say that interaction of the channel i is not the origin. Thus, by taking the ZCL and studying whether the pole remains in the amplitude or not, the origin of dynamically generated poles can be distinguished. If one has the model of the scattering amplitude, this relation between the behavior of the pole in the ZCL and origin of the eigenstate can be utilized as the method to study the structureof the eigenstate. With this method, the

[1] If the system has a symmetry and the interaction of another channel j has the same interaction; $V_{ii} = V_{jj}$, the pole remains in the two components. In the following, we do not consider such a case and we assume that the pole remains at most one components.

structure of $\Lambda(1405)$ has been studied in Ref. [75,76]. The idea of the ZCL is also used in order to extract the nature of the scattering effect of the channel of interest by suppressing the decay effect the in Ref [77]. However, for the application of this method, we need a model for the scattering amplitude to take a ZCL. In the next section, we consider a method to distinguish the behavior of poles in the ZCL from the amplitude without taking the ZCL.

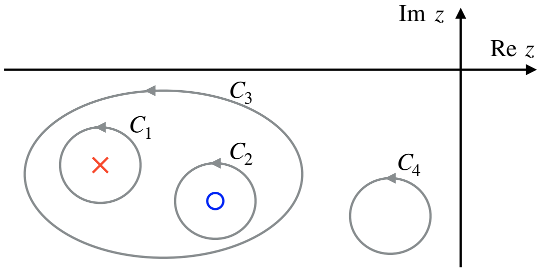

Figure 3.1: Examples of the closed contour in the complex energy plane. The blue circle and red close denote the zero and the pole of the amplitude, respectively. For each contour, $n_{C_1} = -1$, $n_{C_2} = +1$, and $n_{C_3} = n_{C_4} = 0$.

3.2 Topological discussion

Here we show that the behavior of the poles in the ZCL is related to the position of the CDD zero. Now we consider one component of the coupled channel amplitude. Firstly, we introduce the quantity n_C defined with the analytically continued partial-wave scattering amplitude $\mathscr{F}(z)$ with the complex energy variable z as

$$n_C \equiv \frac{1}{2\pi} \oint_C dz \frac{d \arg \mathscr{F}(z)}{dz}, \tag{3.2.1}$$

where C denotes the counterclockwise closed contour on which $\mathscr{F}(z)$ is analytic. The argument principle leads to

$$n_C = n_Z - n_P \in \mathbb{Z}, \tag{3.2.2}$$

where the integers n_Z and n_P are the numbers of zeros and poles of order 1 of $\mathscr{F}(z)$ enclosed by C (See Fig. 3.1 for illustration.).[2] This is nothing but a topological invariant of $\pi_1(\mathrm{U}(1)) \cong \mathbb{Z}$.

By varying the parameters of the system (e.g. reducing the channel couplings toward the ZCL), the poles and zeros move continuously in the complex z plane and make trajectories. Due to the fact that n_C is the topological invariant, the value of n_C cannot change without the intersection of the trajectories. This topological nature prohibits the abrupt emergence or disappearance of a pole or a zero by itself because such transition changes

[2]If we have a n-th order pole (zero), we count it as n single poles (zeros).

the value of n_C. On the other hand, a pair of pole and zero can emerge or disappear at the same energy point because it keeps the value of n_C.

As we have discussed in Sect. 3.1, the pole with the hidden channel origin must decouple from the scattering amplitude $\mathscr{F}_{ii}$ in the ZCL. The topological nature of the scattering amplitude requires that such pole must encounter with a CDD zero at the energy where the pole decouples in this limit. This means that, with the finite channel couplings, the pole with the hidden channel origin must be accompanied by a CDD zero. The position of the CDD zero must be close to the position of the pole if the coupling is not so strong and the system is close to the ZCL. On the other hand, the pole with dynamical origin of channel i does not need such zero because it remains in $\mathscr{F}_{ii}$ in the ZCL. Then we find a simple relation between the origin of the eigenstate and positions of the poles and zeros:

1. If there is no CDD zero near to the pole in $\mathscr{F}_{ii}(z)$, the eigenstate is dynamically generated in channel i.

2. If the pole is accompanied by a nearby CDD zero, the origin of the eigenstate is not in channel i.

Because this relation is obtained without any conditions but with the fundamental topological nature of the scattering amplitude, it holds for the any eigenstates, e.g. a higher-partial wave state or a deeply bound state. Furthermore, the positions of the poles and zeros are, in principle, uniquely determined and therefore they are model-independent quantities. Thus, by studying the positions of the poles and zeros of the amplitude, we can model-independently discuss the origin of the eigenstate.

3.3 ZCL in effective field theory

In this section, we check how above relation holds in more detail with the solvable model. We employ the non-relativistic field theory, which has been utilized in the study on the weak-binding relation in Chap. 2, as a model and check the behavior of the poles and CDD zeros in the ZCL.

Firstly, let us consider the s-wave scattering problem described by Eq. (2.1.1), where one scattering channel and one discrete channel are coupled with the coupling constant g_0. In this system, the discrete channel can be regarded as the hidden channel. With the scattering amplitude Eq. (2.1.21), we can write down the condition for the E_{pole} as

$$(E_{\text{pole}} - \omega_0)[1 - v_0 G(E_{\text{pole}})] - g_0^2 G(E_{\text{pole}}) = 0, \tag{3.3.1}$$

where the ω_0 is the mass of the discrete state, v_0 is the coupling constant of the four-point interaction of the scattering channel and $G(E)$ is the loop function. The residue of the pole g^2 defined in Eq. (2.1.24) is explicitly written as

$$g^2 = \frac{v_0(E_{\text{pole}} - \omega_0) + g_0^2}{1 - v_0 \left[G(E_{\text{pole}}) + (E_{\text{pole}} - \omega_0)G'(E_{\text{pole}})\right] + g_0^2 G'(E_{\text{pole}})}. \tag{3.3.2}$$

From the numerator of amplitude (2.1.21), the position of the CDD zero E_{CDD} is obtained as

$$E_{\text{CDD}} = \omega_0 - g_0^2/v_0. \tag{3.3.3}$$

Let us examine the behavior of the poles and zeros in this model. Because the discrete channel and the scattering channel is coupled via the coupling constant g_0, the ZCL of this model corresponds to the limit of $g_0 \to 0$. In this limit, Eq. (3.3.1) reduces to

$$(E_{\text{pole}} - \omega_0)[1 - v_0 G(E_{\text{pole}})] = 0, \tag{3.3.4}$$

which implies that there are two possibilities for the behavior of the pole in the ZCL; $E_{\text{pole}} \to \omega_0$ or E_0 with $1 - v_0 G(E_0) = 0$. In the former case, the pole originates in the discrete channel because the position in the ZCL is determined only by the mass of the discrete state. In the latter case, the dynamical channel is the origin because the position of the pole in the ZCL is determined by the dynamics of the scattering channel. On the other hand, the CDD zero always behaves as $E_{\text{CDD}} \to \omega_0$.

Now we check the relation between the origin of eigenstate and the positions of the poles and zeros. The pole with the discrete channel origin encounters with the CDD zero at $E = \omega_0$ in the ZCL. By the cancel of the zero of the denominator and the zero of the numerator, the pole and the CDD zero no longer exist in the exact ZCL ($g_0 = 0$). The annihilation of the pole can be also checked by the vanishing of the residue of the pole: $g^2 \to 0$. From Eqs. (3.3.1) and (3.3.3), the distance between the pole and the zero is written as

$$E_{\text{pole}} - E_{\text{CDD}} = \frac{g_0^2}{\left[1 - v_0 G(E_{\text{pole}})\right] v_0}, \tag{3.3.5}$$

which is of the order of g_0^2. This means that, when the coupling constant is small, the distance between the pole and zero is also small and the CDD zero must lie near to the eigenstate pole. When the pole has the dynamical origin, the destination of the pole is independent of that of the CDD zero. In this case, the position of the CDD zero with finite channel couplings can be far from the eigenstate pole.

Next, let us consider the system with two scattering channels. For this system, we employ the Hamiltonian given in Eqs. (2.2.1)-(2.2.3) with $g_{0,1} = g_{0,2} = 0$. The interaction of these channels are written by the 2×2 matrix as

$$V = \begin{pmatrix} v_{0,11} & v_{0,12} \\ v_{0,21} & v_{0,22} \end{pmatrix}. \tag{3.3.6}$$

Channel 2 is regarded as the hidden channel from channel 1. By taking $g_{0,i} = 0$ in Eq. (3.3.7), the scattering amplitude of channel 1 can be explicitly written as

$$t_{11}(E) = \frac{v_{0,11}[1 - v_{0,22}G_2] + v_{0,12}^2 G_2}{[1 - v_{0,11}G_1][1 - v_{0,22}G_2] - v_{0,12}^2 G_1 G_2}. \tag{3.3.7}$$

With this amplitude, the conditions for the pole E_{pole} and the CDD zero of the amplitude of channel 1 E_{CDD} are given as

$$(1 - v_{0,11}G_1(E_{\text{pole}}))(1 - v_{0,22}G_2(E_{\text{pole}})) - v_{0,12}^2 G_1(E_{\text{pole}}) G_2(E_{\text{pole}}) = 0, \tag{3.3.8}$$

$$v_{0,11}[1 - v_{0,22}G_2(E_{\text{CDD}})] + v_{0,12}^2 G_2(E_{\text{CDD}}) = 0. \tag{3.3.9}$$

In this model, the ZCL corresponds to the limit of $v_{0,12} \to 0$. In this limit, the condition for the pole (3.3.8) reduces to

$$\left[1 - v_{0,11}G_1(E_{\text{pole}})\right]\left[1 - v_{0,22}G_2(E_{\text{pole}})\right] = 0. \tag{3.3.10}$$

the eigenstate pole behaves as $E_{\text{pole}} \to E_{0,1}$ or $E_{0,2}$ with $1 - v_{0,11}G_1(E_{0,1}) = 0$ and $1 - v_{0,22}G_2(E_{0,2}) = 0$. In the former (latter) case, the eigenstate pole originates in channel 1 (2) because its position is determined only by the dynamics of channel 1 (2). In the latter case, the destination of the CDD zero is the same as that of the pole because the condition for the CDD zero (3.3.9) reduces to

$$1 - v_{0,22}G_2(E_{\text{CDD}}) = 0, \tag{3.3.11}$$

which implies that the CDD zero moves to $E_{0,2}$ in both cases. If the eigenstate originates in channel 2, the pole and the CDD zero encounter with each other and both decouple from the scattering amplitude $\sqcup_{11}$. The distance between the pole and CDD zero $E_{\text{pole}} - E_{\text{CDD}}$ is of the order of the square of the coupling constant $\mathscr{O}(v_{0,12}^2)$.If the coupling $v_{0,12}$ is small, the deviation is also small. As in the case of the origin of the discrete channel, the eigenstate pole emerges with a nearby CDD zero if the channel other than the channel of interest is the origin of the eigenstate.

In this section, we have checked the behavior of the pole and CDD zero in the ZCL within the nonrelativistic field theory. As expected from the discussion in Sect. 3.2, we have seen that the eigenstate pole originated in the hidden channel decouples from the amplitude by encountering the CDD zero in the ZCL. The distance of the pole and zero is determined by the hidden channel in both case. The deviation between the pole and CDD zero is of the order of the square of the coupling constant between the hidden channel and the channel of interest. Thus, in both cases, the nearby CDD zero emerges when the origin of the eigenstate is in the hidden channel.

3.4 Summary

In this chapter, we have shown the relation between the origin of the eigenstate and the positions of the eigenstate pole and CDD zero. This relation is summarized in Table 3.1. With this relation, we can interpret the CDD zero of the scattering amplitude as the contribution from the hidden channel. This relation gives us the method to distinguish the origin of the eigenstate by searching the positions of the pole and the CDD zero in the complex energy plane. If one has the two-body scattering amplitude (e.g. obtained by analyzing the sufficiently accurate experimental data of final state interactions), the positions of the eigenstate pole and the CDD zero can be identified. Then the origin of the eigenstate can be distinguished from the presence or absence of the nearby CDD zero.

Compared to the method utilizing the weak-binding relation which we have discussed in Chapter 2, this method has the broad applicability because it can be applied to eigenstates in higher-partial waves or deeply bound states, to which the weak-binding relation cannot be applied. This is because the method is constructed based on the topological nature of the amplitude. We note that this method only gives the qualitative result about the structure, while we can obtain the quantitative result of the compositeness by applying the weak-binding relation.

Both the method utilizing the position of CDD zero and the pole counting rule [67,68] discussed in Sect. 1.2.4 utilizes the analytic structure of the scattering amplitude to discuss the origin of the eigenstate. As shown in Table 3.1, our method utilizes the position of the zero while the pole counting rule utilizes the position of the shadow pole. However, there two differences. One of them is that the pole counting rule can be utilized only for

Table 3.1: Relation between the origin of the eigenstate and the presence or absence of the nearby CDD zero. We also summarize the relation between the origin and the presence or absence of the shadow pole in the near-threshold energy region.

Origin of the eigenstate	Nearby CDD zero	Shadow pole
Scattering channel of interest	Absence	Absence
Hidden channel	Presence	Presence

the s-wave near-threshold state while the method discussed here can be applied to any eigenstates. The other is that while the CDD zero lies in the most adjacent Riemann sheet to the real axis as the eigenstate pole does, the shadow poles exist in Riemann sheets which are not directly connected to the real axis. Thus, it is an advantage of the present method to utilize the position of the CDD zero which can be determined less ambiguously than those of the shadow poles. Moreover, the CDD zero can appear on the real axis as in the $\pi\Sigma$ scattering amplitude [52] as shown in Fig. 1.5 and in the $I = 0$ $\pi\pi$ scattering amplitude near the $\bar{K}K$ threshold [78].

From these considerations, we can say that the present method is suitable to study structure of the exotic hadron candidates. Thus, we consider that this method facilitates the future investigation of the hadron structure. We will discuss the application of this method to actual hadrons in Chapter 4.

Chapter 4

Application to Hadrons

In the previous chapters, we have constructed two methods to discuss the structure of hadrons from the scattering amplitude. In Chapter 2, the method to evaluate the compositeness of hadrons states has been constructed by extending the weak-binding relation to the general cases. In Chapter 3, we have proposed the method to distinguish the origin of hadron states from the position of the eigenstate pole and CDD zero. In this chapter, we apply these methods to some hadron systems to discuss the structure that emerges in the system.

4.1 Compositeness

As discussed, the extended weak-binding relation can be applied to the hadrons that lie near threshold. First of all, we revisit the case of the deuteron in the proton-neutron scattering. After that we discuss the applications to the exotic hadron candidates, $\Lambda(1405)$, light scalar mesons, and $N\Omega$ quasibound state.

4.1.1 Deuteron

For now, the deuteron is the unique state known as the two-body hadron composite state. In addition, as far as we know, the only state to which the original weak-binding relation is applicable is the deuteron. Thus, to check how the weak-binding relation works for this state is a good starting point before we discuss the structure of exotic candidates.

The threshold parameters of the proton-neutron scattering in $^3S_1$ and the binding energy of the deuteron are determined with sufficient accuracy to apply the weak-binding relation, as follows [79, 80],

$$a_0 = 5.419 \pm 0.007 \text{ fm}, \tag{4.1.1}$$

$$r_e = 1.7513 \pm 0.008 \text{ fm}, \tag{4.1.2}$$

$$B = 2.224575 \pm 0.000009 \text{ MeV}. \tag{4.1.3}$$

In the following, we only utilize the central value of these quantities. The length scale R is calculated as $R = 1/\sqrt{2\mu B} = 4.31767$ fm, where μ is the reduced mass of the p-n system. Because the π meson is the lightest meson that can be exchanged, the typical length scale $R_{\rm typ}$ can be estimated from the exchange of the π meson as

$$R_{\rm typ} = 1/m_\pi \sim 1.43 \text{ fm}. \tag{4.1.4}$$

This gives the magnitude of the correction term as $R_{\rm typ}/R \sim 0.33$. Because this value is less than unity but not so small that the correction term is negligible, we have to apply the weak-binding relation paying attention to the contribution of the correction term.

Now using the Eqs. (2.1.45) and (2.1.46), the np compositeness and its error arising from the correction term of weak-binding relation is obtained as

$$X = 1.68^{+2.15}_{-0.82} \tag{4.1.5}$$

One can see that the central value of the compositeness exceeds unity. This value seems, at first sight, to contradict the fact that the compositeness of a stable state is bounded in $[0, 1]$. This value is caused by the large contribution from the correction term $\mathcal{O}(R_{\rm typ}/R)$, that also leads to the large error of the compositeness. However, taking this error into account, the lower boundary of the compositeness is 0.86. This means that the compositeness is consistent with the scenario where the deuteron is the molecular state of the proton and neutron, $X \sim 1$, while the other scenario, $X \sim 0$, is not realistic. Thus we safely conclude that the deuteron is a n-p composite state.

Within this case, we have seen that determination of structure with the weak-binding relation using the experimental observables works well for an actual hadron. It is also found that appropriate evaluation of the contribution from the correction term is necessary for the conclusion.

Table 4.1: Properties and results for the high-mass pole of $\Lambda(1405)$ shown are the eigenenergy E_h, the $\bar{K}N(I=0)$ scattering length a_0, the $\bar{K}N$ compositeness $X_{\bar{K}N}$ and $\tilde{X}_{\bar{K}N}$ and the uncertainty of the interpretation $U/2$.

	E_h [MeV]	a_0 [fm]	$X_{\bar{K}N}$	$\tilde{X}_{\bar{K}N}$	$U/2$
Set 1 [59]	$-10-i26$	$1.39-i0.85$	$1.2+i0.1$	1.0	0.3
Set 2 [82]	$-\ 4-i\ 8$	$1.81-i0.92$	$0.6+i0.1$	0.6	0.0
Set 3 [83]	$-13-i20$	$1.30-i0.85$	$0.9-i0.2$	0.9	0.1
Set 4 [84]	$2-i10$	$1.21-i1.47$	$0.6+i0.0$	0.6	0.0
Set 5 [84]	$-\ 3-i12$	$1.52-i1.85$	$1.0+i0.5$	0.8	0.3

4.1.2 $\Lambda(1405)$

From here on, we start to apply the extended relation for the unstable state to the exotic candidates. The first target is the $\Lambda(1405)$. This state is unstable due to the decay mode to the $\pi\Sigma$ channel. Among the two poles of $\Lambda(1405)$, high-mass pole lies close to the $\bar{K}N$ threshold. On the other hand, none of the threshold that couple to the $\Lambda(1405)$ is close to the low-mass pole. Thus the $\bar{K}N$ compositeness of the high-mass pole can be discussed using the extended weak-binding relation.

To apply the weak-binding relation, we need the $I=0$ scattering length and the pole position of the high-mass pole. Though, in principle, these values can be uniquely determined with the detailed analysis of the sufficient data, they are still different in the recent analyses. So we employ the results of the analyses to estimate the systematic error. In the recent study, the most systematic analysis of the $\bar{K}N$ scattering amplitude is proceeded with the chiral unitary method [59,81–84], whose results are summarized in the table 4.1.

Let us check the magnitude of the higher-order terms $\mathscr{O}(|R_{\rm typ}/R|)$ and $\mathscr{O}(|l/R|^3)$ in the extended weak-binding relation. From Table 4.1, we see that the absolute value of the eigenenergy in all cases satisfies $|E_h| \lesssim 28$ MeV, which leads to $|R| \gtrsim 1.5$ fm. We estimate the typical length scale $R_{\rm typ}$ from the mass of the ρ meson as $R_{\rm typ} = 1/m_\rho \sim 0.25$ fm. This is because the lightest meson π cannot be exchanged due to the parity conservation and the σ meson has a large width. The difference of the threshold energy of the $\bar{K}N$ channel and that of the $\pi\Sigma$ channel is calculated as $\omega = 104$ MeV, which

Table 4.2: The results of error evaluation of the compositeness $\tilde{X}_{\bar{K}N}$ of $\Lambda(1405)$ with the value of $|R_{\rm typ}/R|$ and $|l/R|^3$.

	$\lvert R_{\rm typ}/R\rvert$	$\lvert l/R\rvert^3$	$\tilde{X}_{\bar{K}N}$
Set 1 [59]	0.17	0.14	$1.0^{+0.0}_{-0.4}$
Set 2 [82]	0.10	0.03	$0.6^{+0.2}_{-0.1}$
Set 3 [83]	0.16	0.11	$0.9^{+0.1}_{-0.4}$
Set 4 [84]	0.10	0.03	$0.6^{+0.3}_{-0.1}$
Set 5 [84]	0.12	0.04	$0.8^{+0.2}_{-0.2}$

leads to the length scale $l = 1/\sqrt{2\mu\omega} = 0.76$ fm. With these values, the magnitude of the higher-order terms in the weak-binding relation is estimated as $|R_{\rm typ}/R| \lesssim 0.17$ and $|l/R|^3 \lesssim 0.14$. We find that these values are not sufficiently small to estimate the compositeness by the weak-binding relation.

By neglecting the higher-order terms, the central value of the compositeness $X_{\bar{K}N}$, $\tilde{X}_{\bar{K}N}$ and the uncertainty of the interpretation $U/2$ are calculated for each set. We summarize the results in Table 4.1. We find that the value of $U/2$ is much smaller than unity in all sets. This fact allows us to interpret the value of $\tilde{X}_{\bar{K}N}$ as the probability. Then the evaluated central value $\tilde{X}_{\bar{K}N} \sim 1$ in all sets implies that the $\bar{K}N$ composite component is dominant for this eigenstate of $\Lambda(1405)$.

Next, employing the method constructed in Sect. 2.2.6, we evaluate the uncertainty of $\tilde{X}_{\bar{K}N}$ that comes from the higher-order terms in the weak-binding relation. By varying the value of ξ_c in the region $|\xi_c| \leq |R_{\rm typ}/R| + |l/R|^3$, we obtain the uncertainty band of $\tilde{X}_{\bar{K}N}$. The results are summarized in Table 4.2 and graphically shown in Fig. 4.1. We find that $\tilde{X}_{\bar{K}N}$ is larger than 0.5 even if the uncertainty band is taken into account. Thus we finally conclude that the structure of the eigenstate represented by the high-mass pole is dominated by the $\bar{K}N$ composite component.

We note that the deviation of the value of the compositeness among different sets is caused by deviation of the eigenenergy and the scattering length in these analyses. Improving the analyses method togather with the quality of the experimental data, the uncertainty of the values of a_0 and E_h will be decreased and the deviation of the calculated

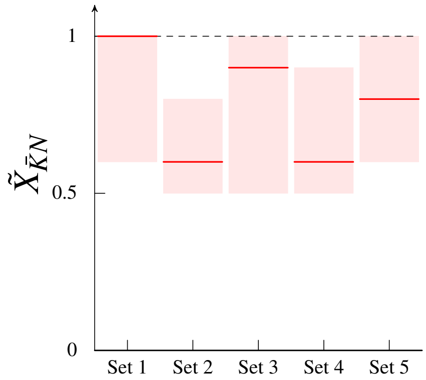

Figure 4.1: The results of error evaluation of the compositeness $\tilde{X}_{\bar{K}N}$ of $\Lambda(1405)$. The lines denote the central values and the shaded areas indicate the uncertainty bands.

$\tilde{X}$ will be reduced.

We also check the CDD zero contribution to $\Lambda(1405)$. To apply the extended weak-binding relation (2.3.7), we additionally need the effective range of the $I = 0$ $\bar{K}N$ amplitude. We use the $a_0 = 1.39 - i0.85$ fm, $r_e = 0.24 - i0.05$ fm and $E_h = -10 - i26$ MeV obtained in the analysis [59]. With these values, the X and $\tilde{X}_{\bar{K}N}$ are calculated as $(X, \tilde{X}_{\bar{K}N}) = (1.4 + i0.2,\ 1.0)$. Both of these values are very close to results obtained in Table 4.1. This means that the CDD zero contribution is negligible and the ERE works well. The CDD zero contribution to $\Lambda(1405)$ will be further discussed in Sect. 4.2.1.

4.1.3 Scalar mesons

We discuss the structure of the scalar mesons $f_0(980)$ and $a_0(980)$, which have isospin $I = 0$ and 1 and have the decay mode to $\pi\pi$ channel and $\pi\eta$ channel, respectively. Because both states lie close to the $\bar{K}K$ threshold, we discuss the $\bar{K}K$ compositeness of these states. To calculate the compositeness, we use the isospin-averaged mass for the $\bar{K}K$ channel. Using the Flatté amplitude [85], the $\bar{K}K$ amplitude is analyzed in Refs. [86–96]. These analyses mainly utilized the experimental data of the heavy meson decay spectra. The eigenenergies of $f_0(980)$ and $a_0(980)$ and the scattering length of the $\bar{K}K(I = 0)$ and $\bar{K}K(I = 1)$ channels obtained from these Flatté amplitudes are summarized in Tables 4.3

Table 4.3: Properties and results for $f_0(980)$ shown are the eigenenergy E_h, $\bar{K}K(I=0)$ scattering length a_0, the $\bar{K}K$ compositeness $X_{\bar{K}K}$ and $\tilde{X}_{\bar{K}K}$ and the uncertainty of the interpretation U.

Ref.	E_h [MeV]	a_0 [fm]	$X_{\bar{K}K}$	$\tilde{X}_{\bar{K}K}$	$U/2$
[86]	$19-i30$	$0.02-i0.95$	$0.3-i0.3$	0.4	0.1
[87]	$-6-i10$	$0.84-i0.85$	$0.3-i0.1$	0.3	0.0
[88]	$-8-i28$	$0.64-i0.83$	$0.4-i0.2$	0.4	0.0
[89]	$10-i18$	$0.51-i1.58$	$0.7-i0.3$	0.6	0.1
[90]	$-10-i29$	$0.49-i0.67$	$0.3-i0.1$	0.3	0.0
[91]	$10-i\ 7$	$0.52-i2.41$	$0.9-i0.2$	0.9	0.1

and 4.4, respectively.

Now let us estimate the magnitude of higher-order terms in the weak-binding relation. The typical length scale R_{typ} can be estimated from the mass of ρ meson as $R_{\text{typ}} \sim 1/m_\rho$. The length scale l is determined as $l = 0.33$ fm ($l = 0.51$ fm) from the difference between the threshold energies $\omega = 715$ MeV ($\omega = 305$ MeV) for the $I=0$ $\pi\pi$ ($I=1$ $\pi\eta$) channel. Except for the eigenenergy obtained in Ref. [92], the eigenenergies satisfy $|R| \gtrsim 1.5$ fm, which leads $|R_{\text{typ}}/R| \lesssim 0.17$ and $|l/R|^3 \lesssim 0.04$. With the eigenenergy obtained in Ref. [92], we obtain relatively large values: $|R_{\text{typ}}/R| \sim 0.25$ and $|l/R|^3 \sim 0.13$.

Let us discuss the structure of $f_0(980)$ firstly. The calculated compositeness $X_{\bar{K}K}$, $\tilde{X}_{\bar{K}K}$ and $U/2$ are summarized in Table 4.3. The estimated errors of $\tilde{X}_{\bar{K}K}$ are summarized in Table 4.5 and graphically shown in Fig. 4.2. Because the uncertainty of the interpretation is small as $U/2 \leq 0.1$ for all cases, the values of $\tilde{X}_{\bar{K}K}$ can be considered as the probabilities. However, the central values of the compositeness $\tilde{X}_{\bar{K}K}$ are very scattered. Even though we take error into account, we cannot find the consistent value in all cases. Thus we cannot determine whether the $\bar{K}K$ composite component is dominant or not. This is caused by the sizable deviation among E_h and a_0 obtained by the analyses in Refs. [86–91]. Reducing the ambiguity of theses values with the improved analyses together with the experimental data, we can discuss the structure of this eigenstate from the value of the compositeness if the obtained eigenenergy is close to the $K\bar{K}$ threshold energy.

Table 4.4: Properties and results for $a_0(980)$ shown are the eigenenergy E_h, $\bar{K}K(I=1)$ scattering length a_0, the $\bar{K}K$ compositeness $X_{\bar{K}K}$ and $\tilde{X}_{\bar{K}K}$ and the uncertainty of the interpretation U.

Ref.	E_h [MeV]	a_0 [fm]	$X_{\bar{K}K}$	$\tilde{X}_{\bar{K}K}$	$U/2$
[92]	$31-i70$	$-0.03-i0.53$	$0.2-i0.2$	0.3	0.1
[93]	$3-i25$	$0.17-i0.77$	$0.2-i0.2$	0.2	0.0
[94]	$9-i36$	$0.05-i0.63$	$0.2-i0.2$	0.2	0.0
[95]	$14-i\ 5$	$-0.13-i2.19$	$0.8-i0.4$	0.7	0.1
[96]	$15-i29$	$-0.13-i0.52$	$0.1-i0.2$	0.1	0.0

Next, let us discuss the structure of $a_0(980)$. The results of the compositeness are summarized in Table 4.4 and Fig 4.3. The values of $U/2$ are again small enough in all cases and we can regard the values of $\tilde{X}$ as the probabilities. The values of $\tilde{X}_{\bar{K}K}$ for Ref. [93, 94, 96] are close to zero. For Ref. [92], due to the relatively large values of $|R_{\rm typ}/R|$ and $|l/R|^3$, the estimated $\tilde{X}_{\bar{K}K}$ has large uncertainty band. However, taking into account its uncertainty, the value is consistent with the above three cases. The large value of $\tilde{X}_{\bar{K}K}$ with the analysis in Ref. [95] looks inconsistent with the others. Up to this point, we have utilized the central values of the Flatté parameters to calculate the eigenenergies and scattering length while the Flatté parameters obtained in each analysis also have the finite uncertainties. The uncertainty of the $\bar{K}K$ coupling constant, which is one of the Flatté parameters, in Ref. [95] is sizably larger than those in the other analyses. By taking into account this uncertainty of the parameter, the compositeness of $\tilde{X}_{\bar{K}K}$ for Ref. [95] is obtained as $\tilde{X}_{\bar{K}K}=0.7^{+0.1}_{-0.7}$, which is consistent with the other results. Considering from these results, we conclude that the $\bar{K}K$ dynamical state is not the dominant component in $a_0(980)$. The possible candidates of the structure of this state are, for example, the simple $q\bar{q}$ configuration, the tetraquark state $qq\bar{q}\bar{q}$ or the other composite state such as $\pi\eta$.

4.1.4 $N\Omega$ dibaryon

Here we discuss the $N\Omega$ compositeness of the $N\Omega$ dibaryon, which is the bound state of the nucleon and the Ω baryon. The recent lattice QCD calculation using the so-called

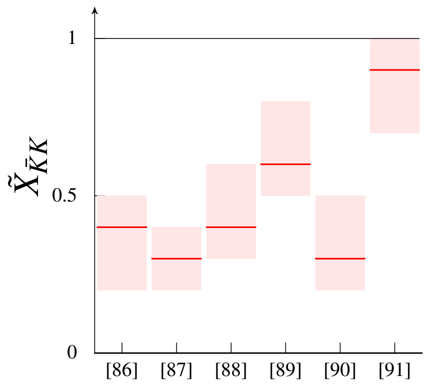

Figure 4.2: The results of error evaluation of the compositeness $\tilde{X}_{\bar{K}K}$ of $f_0(980)$. The lines denote the central values and the shaded areas indicate the uncertainty bands.

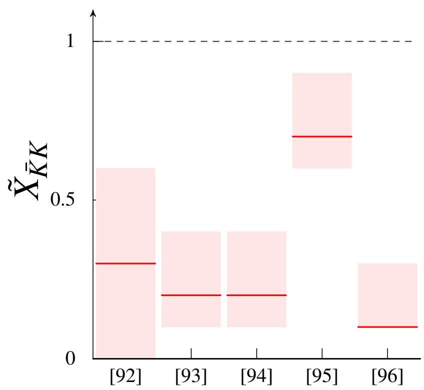

Figure 4.3: The results of error evaluation of the compositeness $\tilde{X}_{\bar{K}K}$ of $a_0(980)$. The lines denote the central values and the shaded areas indicate the uncertainty bands.

Table 4.5: The results of error evaluation of the compositeness $\tilde{X}_{\bar{K}K}$ of $f_0(980)$ with the value of $|R_{\rm typ}/R|$ and $|l/R|^3$.

Ref.	$\lvert R_{\rm typ}/R\rvert$	$\lvert l/R\rvert^3$	$\tilde{X}_{\bar{K}K}$
[86]	0.17	0.00	$0.4^{+0.1}_{-0.2}$
[87]	0.01	0.00	$0.3^{+0.1}_{-0.1}$
[88]	0.15	0.01	$0.4^{+0.2}_{-0.1}$
[89]	0.13	0.01	$0.6^{+0.2}_{-0.1}$
[90]	0.16	0.01	$0.3^{+0.2}_{-0.1}$
[91]	0.10	0.00	$0.9^{+0.1}_{-0.2}$

Table 4.6: The results of error evaluation of the compositeness $\tilde{X}_{\bar{K}K}$ of $a_0(980)$ with the value of $|R_{\rm typ}/R|$ and $|l/R|^3$.

Ref.	$\lvert R_{\rm typ}/R\rvert$	$\lvert l/R\rvert^3$	$\tilde{X}_{\bar{K}K}$
[92]	0.25	0.13	$0.3^{+0.3}_{-0.3}$
[93]	0.14	0.02	$0.2^{+0.2}_{-0.1}$
[94]	0.17	0.04	$0.2^{+0.2}_{-0.1}$
[95]	0.11	0.01	$0.7^{+0.2}_{-0.1}$
[96]	0.16	0.04	$0.1^{+0.2}_{-0.0}$

HAL QCD method [97,98] suggests the weakly-bound $N\Omega$ state. Stimulated to this result, the $N\Omega$ interaction is studied within the framework of the chiral perturbation theory [99] and meson exchange model [100].

In the latest result of the HAL QCD calculation with the almost physical quark mass $m_\pi = 146$ MeV is reported in Ref. [97]. The binding energy and the scattering length are obtained as $E_h = -1.54$ MeV and $a_0 = 5.30$ fm.[1] Using these values and Eq. (2.1.37),

[1] In this study, by assuming that the coupling between the $N\Omega$ channel and the decay channels of $\Sigma\Xi$ and $\Lambda\Xi$ is kinematically suppressed, the analysis is done in a single channel framework. In fact, in Ref. [100], it is pointed out that the effect of coupling to these channels is small.

the compositeness of the $N\Omega$ dibaryon is calculated as

$$X = 1.4^{+0.5}_{-0.4}, \tag{4.1.6}$$

where the magnitude of the correction term can be estimated as $|R_{\rm typ}/R| \sim 0.1$ from the 2π exchange interaction.[2] This results suggests the molecular picture of N and Ω.

The analysis including the decay modes is done in Ref. [100]. In this study, the long range part of the interaction is given by the meson exchange mechanism and the short range part is given by the contact interaction which is tuned to reproduce the scattering length of the HAL QCD result. The coupled-channel effect is taken into account

The eigenenergy and scattering length are obtained as $E_h = -0.1 - i0.7$ MeV and $a_0 = 5.3 - i4.3$ fm. The magnitude of the correction term can be estimated as $|R_{\rm typ}/R| \sim 0.1$ and $|l/R|^3 \sim 0.0$, where we have used $l = 0.57$ MeV calculated from the difference of the threshold energy between $N\Omega$ and $\Sigma\Xi$. By utilizing these values, $X_{N\Omega}$, $\tilde{X}_{N\Omega}$ and U are calculated as

$$X_{N\Omega} = 1.1 + 0.1i, \quad \tilde{X}_{N\Omega} = 1.0^{+0.0}_{-0.1}, \quad U = 0.1. \tag{4.1.7}$$

This results also suggests that the structure of $N\Omega$ dibaryon is dominated by the molecular state of N and Ω.

[2]Here, we have used the weak-binding relation for the stable state because the scattering length and binding energy are calculated within the single channel framework and they are real. However, $N\Omega$ dibaryon can decay to lower energy channels. Thus using the relation for the stable state is an approximation.

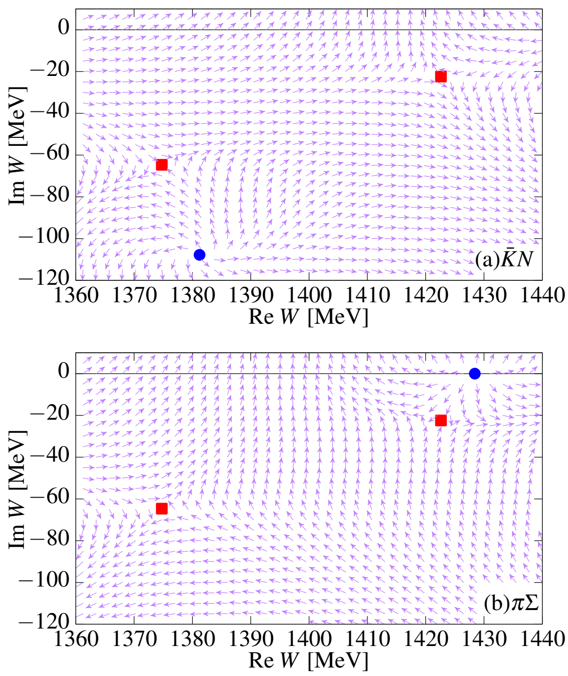

Figure 4.4: Positions of the poles (squares) and CDD zeros (circles) in the $\bar{K}N$ amplitude (a) and the $\pi\Sigma$ amplitude (b). The angle of vectors from the real axis denotes the phase of amplitude $\arg \mathscr{F}_{ii}(z)$.

4.2 Poles and zeros of the amplitude

Next we discuss the origin of hadron resonances from the position of the poles and CDD zeros based on the method developed in Chapter 3. Here we consider the application to $\Lambda(1405)$. In contrast to the weak-binding relation, with this method, we can discuss not only the high-mass pole but also the low-mass pole.

4.2.1 $\Lambda(1405)$

Let us consider the structure of $\Lambda(1405)$ from the zero of the scattering amplitude. To do this, we need to analyze the position of the poles and zeros of the amplitude. Here we employ the Effective Tomozawa-Weinberg (ETW) model [59], that is constructed to reproduce the experimental data around $\bar{K}N$ threshold energy including the SIDDHARTHA constraint using the Tomozawa-Weinberg interaction of the with the $\bar{K}N$, $\pi\Sigma$ and $\pi\Lambda$

Figure 4.5: Examples of the structure of the phase of the amplitude around the pole (left) and around the zero (right).

channels. The Tomozawa-Weinberg interaction is the leading order term of the the chiral perturbation theory and is the energy dependent contact interaction. With the isospin symmetric hadron masses, the two-pole structure of $\Lambda(1405)$ [1,11] is reproduced and the poles are found at

$$W_{\text{pole}}^{\text{Low}} = 1375 - 65i \ \text{MeV}, \tag{4.2.1}$$
$$W_{\text{pole}}^{\text{High}} = 1423 - 22i \ \text{MeV}. \tag{4.2.2}$$

We call $W_{\text{pole}}^{\text{Low}}$ ($W_{\text{pole}}^{\text{High}}$) the low-mass (high-mass) pole.

By analyzing the $\bar{K}N \to \bar{K}N$ and $\pi\Sigma \to \pi\Sigma$ amplitudes in the $\Lambda(1405)$ region, we find two CDD zeros. One lies near the low-mass pole in the $\bar{K}N$ amplitude and the other lies near the high-mass pole in the $\pi\Sigma$ channel. We denote the energy of the former(later) zero as $W_{\text{CDD}}^{\text{Low}}$ ($W_{\text{CDD}}^{\text{High}}$), whose position is found as

$$W_{\text{CDD}}^{\text{Low}} = 1381 - 108i \ \text{MeV}, \tag{4.2.3}$$
$$W_{\text{CDD}}^{\text{High}} = 1428 - 0i \ \text{MeV}, \tag{4.2.4}$$

where $W_{\text{CDD}}^{\text{Low}}$ is in the $\bar{K}N$ amplitude and $W_{\text{CDD}}^{\text{High}}$ is in the $\pi\Sigma$ amplitude. The positions of the poles and CDD zeros are shown in Fig. 4.4 by the red squares and blue circles, respectively. Note that the poles exist at the same position in both channels. First, for the high-mass pole $W_{\text{pole}}^{\text{High}}$, the nearby CDD zero $W_{\text{CDD}}^{\text{High}}$ appears only in the $\pi\Sigma$ amplitude. This means that the origin of the eigenstate represented by the high-mass pole $W_{\text{pole}}^{\text{High}}$ is not the interaction of the $\pi\Sigma$ channel, but that of the $\bar{K}N$ channel. This consequence is consistent with the discussion from the compositeness in Sect. 4.1. Next, around the low-mass pole $W_{\text{pole}}^{\text{Low}}$, the CDD zero $W_{\text{CDD}}^{\text{Low}}$ appears only in the $\pi\Sigma$ amplitude. This implies that the low-mass pole originates in the $\pi\Sigma$ channel. Because the weak-binding relation

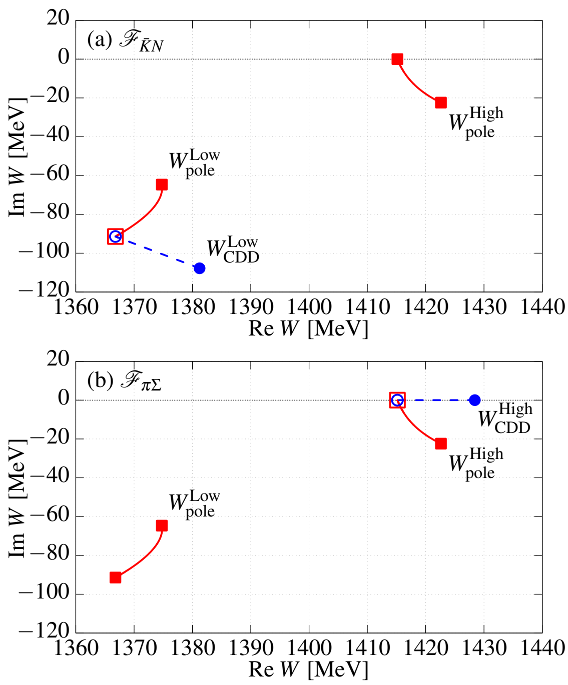

Figure 4.6: Trajectories of poles (solid line) and CDD zeros (dashed line) toward the ZCL in the $\bar{K}N$ amplitude (a) and the $\pi\Sigma$ amplitude (b).

cannot be applied to the low-mass pole, it is an advantage of this approach that the origin of the low-mass pole is clarified.

It is instructive to see the structure of the phase of the amplitude around the pole and zeros. In Fig. 4.4, we show the vector map of the phase of the scattering amplitude $\arg \mathscr{F}(z)$. Along the contour enclosing the CDD zero (pole), the vector of the phase rotates counterclockwise (clockwise), which means that the phase increases (decreases) by 2π (See Fig. 4.5). This rotation of the phase gives the topological invariant n_C in Eq. (3.2.1).

It is also instructive to take the ZCL and check that the poles and zeros behave as expected from the discussion in Chapter 3. By suppressing the off-diagonal interaction $V_{\bar{K}N\text{-}\pi\Sigma} \to 0$ and keeping the diagonal parts $V_{\bar{K}N\text{-}\bar{K}N}$ and $V_{\pi\Sigma\text{-}\pi\Sigma}$ unchanged, the trajectories of the poles and CDD zeros obtained as in Fig. 4.6. In the ZCL, the high-mass pole decouples from the $\pi\Sigma$ amplitude while it remains in the $\bar{K}N$ amplitude as a bound state pole [75]. Correspondingly, $W^{\text{High}}_{\text{CDD}}$ moves on the real axis and annihilates the high-mass pole. On the other hand, the low-mass pole $W^{\text{Low}}_{\text{pole}}$ encounters the CDD zero $W^{\text{Low}}_{\text{CDD}}$ and decouples from the $\bar{K}N$ amplitude while it remains in the $\pi\Sigma$ amplitude as a single-channel resonance. This behavior of the poles and accompanied CDD zeros in the ZCL agrees with the expectation the positions of the pole and the CDD zero.

We can also apply the pole counting method introduced in Sect. 1.2.4 to $\Lambda(1405)$. The poles representing eigenstates $W^{\rm Low}_{\rm pole}$ and $W^{\rm Low}_{\rm pole}$, which have been discussed so far, are on the $(1,2)$ sheet, whose imaginary part of the eigen-momentum of the $\bar{K}N$ channel is positive and that of the $\pi\Sigma$ channel is negative. We call other three sheets in the same manner; $(\text{Im } k_{\bar{K}N}, \text{Im } k_{\pi\Sigma}) = (+,+)$ $(1,1)$ sheet, $(-,+)$ $(2,1)$ sheet and $(-,-)$ (2,2) sheet. Searching the $\Lambda(1405)$ energy region of $\text{Im } W < 0$ in the other Riemann sheets, we find one pole in the $(2,2)$ sheet, whose energy is obtained as

$$W^{\rm Low}_{\rm shadow} = 1392 - 126i \text{ MeV}. \tag{4.2.5}$$

The position of this pole is shown in Fig. 4.7 with the physical poles together. This pole lies close to the low-mass pole in the Riemann sheet which is obtained by changing the sign of the momentum of the $\bar{K}N$ channel from the physical sheet. Because this can be understood as the shadow pole of the low-mass pole, we conclude that the $\bar{K}N$ channel is not the origin of the low-mass pole. Correspondingly, if the high-mass pole originates in the $\pi\Sigma$ channel, a shadow pole appears in the $(2,2)$ sheet which is the sheet obtained by changing the sign of the eigen-momentum of the $\bar{K}N$ channel. The absence of the shadow pole of the high-mass pole in the $(2,2)$ sheet implies that the origin of this pole is the $\bar{K}N$ channel.[3] This result is consistent with that obtained by our method using the position of the CDD zero. As expected from the result, by taking the ZCL, the shadow pole moves toward the energy point where the low-mass pole and its low-mass zero annihilates each other in $(1,2)$ sheet. In the ZCL, the shadow pole in the $\bar{K}N$ amplitude is annihilated by another CDD zero, which lies in the same sheet while the pole in the $\pi\Sigma$ amplitude remains.

[3] Note that the shadow pole of the high-mass pole in the (1,1) sheet, where the appearance of the pole is forbidden, cannot emerge. Thus we cannot discuss the origin of the high-mass pole from the absence or the presence of the shadow pole of $(2,2)$ sheet.

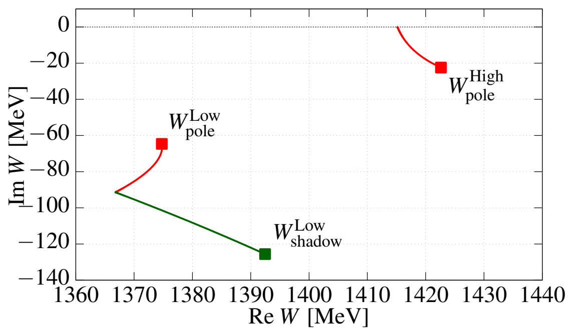

Figure 4.7: Poles of the $\bar{K}N$-$\pi\Sigma$ amplitude in the $\Lambda(1405)$ energy region and their trajectories. The shadow pole, denoted by the green square, is on the $(2,2)$ sheet while the other physical poles are on the $(1,2)$ sheet (see the text for the notation of the Riemann sheet).

4.3 Conclusion

Let us summarize the results of this chapter. Applying the method based on the extended weak-binding relation constructed in Chapter 2 and the method utilizing the positions of poles and CDD zeros constructed in Chapter 3, we have discussed the structure of the actual hadrons. Before discussing the structure of the exotic hadron candidates, we revisit the compositeness of the deuteron and show that the compositeness is qualitatively consistent with the scenario where the deuteron is the n-p composite state if we considered the contribution of the correction term of the weak-binding relation.

By employing the analyses based on the chiral dynamics to know the scattering length and positions of the poles and the CDD zeros, we have found that the state represented by the high-mass pole of the $\Lambda(1405)$ baryon is the $\bar{K}N$ composite state. This is concluded from the compositeness both from the compositeness by the weak-binding relation and from the position of the CDD zero. On the other hand, from the CDD zero position, it has been concluded that the state represented by the low-mass pole originates in the $\pi\Sigma$ interaction. For the scalar mesons, we have utilized the Flatté analyses to calculate the $\bar{K}K$ compositeness and we have concluded that the $\bar{K}K$ compositeness of $a_0(980)$ meson is small. The scattered values of the $\bar{K}K$ compositeness of the $f_0(980)$ meson tells us that the more improved analyses for the isospin $I=0$ $\bar{K}K$ scattering amplitude is needed. With the result of the Lattice QCD calculation and that of the analysis with the meson-exchange interaction model, it is shown that the $N\Omega$ compositeness of the bound state of the $N\Omega$ system is close to unity and the $N\Omega$ dibaryon is dominated by the $N\Omega$ composite state.

Chapter 5

Summary

In this thesis, we have developed two methods to distinguish the structure of the candidates of exotic hadrons. One method has been developed by extending the weak-binding relation to the general cases to extend the applicability. The other method has been developed from the discussion of the position of the zero of the scattering amplitude. Both of these are the model-independent methods because the structure of hadrons can be distinguished only from the quantities that can be in principle determined uniquely from the experimental observables.

In Chapter 2, we have discussed the extension of the weak-binding relation to the general cases. By deriving the original weak-binding relation within the nonrelativistic effective field theory, we show that the weak-binding relation has two independent correction terms. One originates from the assumption that the binding energy is sufficiently small compared with the typical energy scale. The other arises from the assumption of the convergence of the effective range expansion. By considering the coupled channel system, the weak-binding relation is extended for the unstable quasibound state. We show that the contribution of the decay channel can be neglected and the compositeness of the quasibound state can be determined only from the experimental observables if the absolute value of the eigenenergy is sufficiently small compared with the difference of the threshold energies. In order to interpret the complex value of the compositeness X, we construct the prescription employing the real-valued compositeness $\tilde{X}$ and the uncertainty of the interpretation $U/2$. The method to estimate the error of the compositeness arising from the correction terms is developed for the applications. We have also discussed the extension of the weak-binding relation to the case where the effective range expansion does not work well. Employing the Padé approximant for the inverse scattering amplitude, the weak-binding relation is extended to include the nearby CDD zero contribution. With the extended weak-binding relation, it is shown that, even if the CDD zero lies close to the threshold, the compositeness of the near-threshold state can be model-independently determined from the experimental observables.

In Chapter 3, we have discussed the relation between the origin of the eigenstate and positions of the poles and CDD zeros in the complex energy plane. By introducing the zero coupling limit of the coupled-channel amplitude, the origin of the eigenstate can be distinguished from the behavior of the pole in the scattering amplitude of the channel of interest in this limit. Based on the topological nature of the phase of the scattering amplitude, it is shown that the pole must encounter with the CDD zero to decouple from the amplitude. This implies that, with the finite coupling, the nearby CDD zero appears in the complex energy plane if the eigenstate originates in the hidden channel. This means that the origin of the eigenstate can be distinguished by the positions of the eigenstate pole and CDD zero in the complex plane. In the end of the chapter, we have discussed two examples where the nearby CDD zero appears within the nonrelativistic field theories; the eigenstate with the discrete channel origin and with the different dynamical channel origin. In both cases, the destination of the CDD zero and the eigenstate pole in the zero coupling limit is determined by the hidden channel. We also see that the distance between the pole and the CDD zero is of the order of the square of the coupling between the scattering channel and the hidden channel, which implies that the difference is small if the coupling is small.

In Chapter 4, we have applied these two methods to the actual hadrons to discuss their structure. As a first step, we revisit the np compositeness of the deuteron with the weak-binding relation. We see that the central value of the compositeness X estimated from the binding energy and the scattering length exceeds unity while the value is consistent with unity considering the error which originates in the correction term of the weak-binding relation. From this discussion,we understand that it is important to take into account the error of the compositeness. After that, we have discussed the structure of the exotic hadrons candidates. From the $\bar{K}N$ compositeness and the CDD zero position in the $\pi\Sigma$-$\bar{K}N$ amplitude, it is concluded that the high-mass state of the $\Lambda(1405)$ baryon is dominated by the $\bar{K}N$ composite component. From the CDD zero in the $\bar{K}N$ amplitude which lies close to the low-mass pole, we conclude that the origin of the low-mass pole is in the interaction of the $\pi\Sigma$ channel. Employing the Flatté analyses of the $I = 1$ and $I = 0$ $\bar{K}K$ amplitude, we have studied the $\bar{K}K$ compositeness of the $a_0(980)$ and $f_0(980)$ meson, respectively. The results for $a_0(980)$ consistently imply that $a_0(980)$ has small $\bar{K}K$ fraction. However we cannot obtain the consistent results for the structure of $f_0(980)$ with the current precision of the experimental data. For the further study for $f_0(980)$, we need the more precise determination of the $I = 0$ $\bar{K}K$scattering amplitude with the improved experimental data. The $N\Omega$ compositeness of the dibaryon with strangeness $S = -3$ and spin-parity $J^P = 2^+$ has been studied with the result of the Lattice QCD calculation and that of the analysis with the meson-exchange interaction model. We have shown that the dibaryon is dominated by the $N\Omega$ composite component.

Bibliography

[1] Particle Data Group, M. Tanabashi *et al.*, Phys. Rev. **D98**, 030001 (2018).

[2] S. Capstick and N. Isgur, Phys. Rev. **D34**, 2809 (1986), [AIP Conf. Proc.132,267(1985)].

[3] L. Ya. Glozman and D. O. Riska, Phys. Rept. **268**, 263 (1996).

[4] N. Isgur and G. Karl, Phys. Rev. **D18**, 4187 (1978).

[5] N. Isgur and G. Karl, Phys. Rev. **D19**, 2653 (1979), [Erratum: Phys. Rev.D23,817(1981)].

[6] R. H. Dalitz and S. F. Tuan, Phys. Rev. Lett. **2**, 425 (1959).

[7] R. H. Dalitz and S. F. Tuan, Annals Phys. **10**, 307 (1960).

[8] M. H. Alston *et al.*, Phys. Rev. Lett. **6**, 698 (1961).

[9] P. J. Fink, Jr., G. He, R. H. Landau, and J. W. Schnick, Phys. Rev. **C41**, 2720 (1990).

[10] J. A. Oller and U. G. Meissner, Phys. Lett. **B500**, 263 (2001).

[11] D. Jido, J. A. Oller, E. Oset, A. Ramos, and U. G. Meissner, Nucl. Phys. **A725**, 181 (2003).

[12] Y. Kamiya *et al.*, Nucl. Phys. **A954**, 41 (2016).

[13] R. L. Jaffe, Phys. Rept. **409**, 1 (2005).

[14] R. L. Jaffe, Phys. Rev. **D15**, 267 (1977).

[15] R. L. Jaffe, Phys. Rev. **D15**, 281 (1977).

[16] J. D. Weinstein and N. Isgur, Phys. Rev. **D41**, 2236 (1990).

[17] J. A. Oller and E. Oset, Nucl. Phys. **A620**, 438 (1997), [Erratum: Nucl. Phys.A652,407(1999)].

[18] P. Minkowski and W. Ochs, Eur. Phys. J. **C39**, 71 (2005).

[19] F. Dyson and N. H. Xuong, Phys. Rev. Lett. **13**, 815 (1964).

[20] R. L. Jaffe, Phys. Rev. Lett. **38**, 195 (1977), [Erratum: Phys. Rev. Lett.38,617(1977)].

[21] E. S. Swanson, AIP Conf. Proc. **870**, 349 (2006), [,349(2006)].

[22] S. L. Olsen, Front. Phys. **10**, 101401 (2015).

[23] A. Hosaka, T. Iijima, K. Miyabayashi, Y. Sakai, and S. Yasui, **2016**, 062C01 (2016).

[24] Belle, S. K. Choi *et al.*, Phys. Rev. Lett. **91**, 262001 (2003).

[25] T. Barnes and S. Godfrey, Phys. Rev. **D69**, 054008 (2004).

[26] CP-PACS, S. Aoki *et al.*, Phys. Rev. Lett. **84**, 238 (2000).

[27] S. Durr *et al.*, Science **322**, 1224 (2008).

[28] S. E. Koonin, Phys. Lett. **70B**, 43 (1977).

[29] S. Pratt, T. Csorgo, and J. Zimanyi, Phys. Rev. **C42**, 2646 (1990).

[30] W. Bauer, C. K. Gelbke, and S. Pratt, Ann. Rev. Nucl. Part. Sci. **42**, 77 (1992).

[31] R. Lednicky and V. L. Lyuboshits, Sov. J. Nucl. Phys. **35**, 770 (1982), [Yad. Fiz.35,1316(1981)].

[32] M. Gmitro, J. Kvasil, R. Lednicky, and V. L. Lyuboshits, Czech. J. Phys. **B36**, 1281 (1986).

[33] R. Lednicky, Phys. Part. Nucl. **40**, 307 (2009).

[34] C. Greiner and B. Muller, Phys. Lett. **B219**, 199 (1989).

[35] R. Lednicky, V. V. Lyuboshits, and V. L. Lyuboshits, Phys. Atomic Nuclei **61**, 2950 (1998).

[36] M. A. Lisa, S. Pratt, R. Soltz, and U. Wiedemann, Ann. Rev. Nucl. Part. Sci. **55**, 357 (2005).

[37] R. Hanbury Brown and R. Q. Twiss, Nature **178**, 1046 (1956).

[38] G. Goldhaber, S. Goldhaber, W.-Y. Lee, and A. Pais, Phys. Rev. **120**, 300 (1960), [,2(1960)].

[39] A. Ohnishi, Y. Hirata, Y. Nara, S. Shinmura, and Y. Akaishi, Nucl. Phys. **A670**, 297 (2000).

[40] K. Morita, T. Furumoto, and A. Ohnishi, Phys. Rev. **C91**, 024916 (2015).

[41] K. Morita, A. Ohnishi, F. Etminan, and T. Hatsuda, Phys. Rev. **C94**, 031901 (2016).

[42] S. Ohnishi, W. Horiuchi, T. Hoshino, K. Miyahara, and T. Hyodo, Phys. Rev. **C95**, 065202 (2017).

[43] ExHIC, S. Cho *et al.*, Prog. Part. Nucl. Phys. **95**, 279 (2017).

[44] T. Hyodo, D. Jido, and A. Hosaka, Phys. Rev. **C78**, 025203 (2008).

[45] T. Hyodo, Int. J. Mod. Phys. **A28**, 1330045 (2013).

[46] J. C. Taylor, Phys. Rev. **117**, 261 (1960).

[47] N. Hokkyo, Prog. Theor. Phys. **33**, 1116 (1965).

[48] J. R. Taylor, *Scattering Theory: The quantum Theory on Nonrelativistic Collisions* (Wiley, New York, 1972).

[49] H. W. Hammer and D. Lee, Annals Phys. **325**, 2212 (2010).

[50] L. Castillejo, R. H. Dalitz, and F. J. Dyson, Phys. Rev. **101**, 453 (1956).

[51] G. F. Chew and S. C. Frautschi, Phys. Rev. **124**, 264 (1961).

[52] Y. Kamiya and T. Hyodo, PTEP **2017**, 023D02 (2017).

[53] J. A. Oller and E. Oset, Phys. Rev. **D60**, 074023 (1999).

[54] U.-G. Meissner and J. A. Oller, Nucl. Phys. **A673**, 311 (2000).

[55] V. Baru, C. Hanhart, Yu. S. Kalashnikova, A. E. Kudryavtsev, and A. V. Nefediev, Eur. Phys. J. **A44**, 93 (2010).

[56] C. Hanhart, Yu. S. Kalashnikova, and A. V. Nefediev, Eur. Phys. J. **A47**, 101 (2011).

[57] Z.-H. Guo and J. A. Oller, Phys. Rev. **D93**, 054014 (2016).

[58] X.-W. Kang and J. A. Oller, Eur. Phys. J. **C77**, 399 (2017).

[59] Y. Ikeda, T. Hyodo, and W. Weise, Nucl. Phys. **A881**, 98 (2012).

[60] S. Weinberg, Phys. Rev. **137**, B672 (1965).

[61] V. Baru, J. Haidenbauer, C. Hanhart, Yu. Kalashnikova, and A. E. Kudryavtsev, Phys. Lett. **B586**, 53 (2004).

[62] T. Hyodo, Phys. Rev. Lett. **111**, 132002 (2013).

[63] T. Hyodo, D. Jido, and A. Hosaka, Phys. Rev. **C85**, 015201 (2012).

[64] F. Aceti and E. Oset, Phys. Rev. **D86**, 014012 (2012).

[65] T. Sekihara, T. Hyodo, and D. Jido, PTEP **2015**, 063D04 (2015).

[66] Y. Tsuchida and T. Hyodo, Phys. Rev. **C97**, 055213 (2018).

[67] D. Morgan and M. R. Pennington, Phys. Lett. **B258**, 444 (1991), [Erratum: Phys. Lett.B269,477(1991)].

[68] D. Morgan, Nucl. Phys. **A543**, 632 (1992).

[69] R. J. Eden and J. R. Taylor, Phys. Rev. **133**, B1575 (1964).

[70] D. B. Kaplan, Nucl. Phys. **B494**, 471 (1997).

[71] E. Braaten, M. Kusunoki, and D. Zhang, Annals Phys. **323**, 1770 (2008).

[72] T. Sekihara, Phys. Rev. **C95**, 025206 (2017).

[73] F. Aceti, L. R. Dai, L. S. Geng, E. Oset, and Y. Zhang, EPJ Web Conf. **73**, 04009 (2014).

[74] B. C. Pearce and B. F. Gibson, Phys. Rev. **C40**, 902 (1989).

[75] T. Hyodo and W. Weise, Phys. Rev. **C77**, 035204 (2008).

[76] A. Cieply, M. Mai, U.-G. Meiner, and J. Smejkal, Nucl. Phys. **A954**, 17 (2016).

[77] U. Raha, Y. Kamiya, S.-I. Ando, and T. Hyodo, Phys. Rev. **C98**, 034002 (2018).

[78] J. R. Pelaez, Phys. Rept. **658**, 1 (2016).

[79] C. Van Der Leun and C. Alderliesten, Nucl. Phys. **A380**, 261 (1982).

[80] R. Machleidt, Phys. Rev. **C63**, 024001 (2001).

[81] Y. Ikeda, T. Hyodo, and W. Weise, Phys. Lett. **B706**, 63 (2011).

[82] M. Mai and U.-G. Meissner, Nucl. Phys. **A900**, 51 (2013).

[83] Z.-H. Guo and J. A. Oller, Phys. Rev. **C87**, 035202 (2013).

[84] M. Mai and U.-G. Meissner, Eur. Phys. J. **A51**, 30 (2015).

[85] S. M. Flatte, Phys. Lett. **B63**, 224 (1976).

[86] CDF, T. Aaltonen *et al.*, Phys. Rev. **D84**, 052012 (2011).

[87] KLOE, F. Ambrosino *et al.*, Phys. Lett. **B634**, 148 (2006).

[88] Belle, A. Garmash *et al.*, Phys. Rev. Lett. **96**, 251803 (2006).

[89] BES, M. Ablikim *et al.*, Phys. Lett. **B607**, 243 (2005).

[90] FOCUS, J. M. Link *et al.*, Phys. Lett. **B610**, 225 (2005).

[91] M. N. Achasov *et al.*, Phys. Lett. **B485**, 349 (2000).

[92] CLEO, G. S. Adams *et al.*, Phys. Rev. **D84**, 112009 (2011).

[93] KLOE, F. Ambrosino *et al.*, Phys. Lett. **B681**, 5 (2009).

[94] D. V. Bugg, Phys. Rev. **D78**, 074023 (2008).

[95] M. N. Achasov *et al.*, Phys. Lett. **B479**, 53 (2000).

[96] E852, S. Teige *et al.*, Phys. Rev. **D59**, 012001 (1999).

[97] HAL QCD, T. Iritani, HAL QCD method and Nucleon-Omega interaction with physical quark masses, in *36th International Symposium on Lattice Field Theory (Lattice 2018) East Lansing, MI, United States, July 22-28, 2018*, 2018.

[98] T. Iritani *et al.*, (2018), 1810.03416.

[99] J. Haidenbauer, S. Petschauer, N. Kaiser, U.-G. Meiner, and W. Weise, Eur. Phys. J. **C77**, 760 (2017).

[100] T. Sekihara, Y. Kamiya, and T. Hyodo, Phys. Rev. **C98**, 015205 (2018).